THE CANADIAN MINERALOGIST

Journal of the Mineralogical Association of Canada

Volume 15 May 1977 Part 2

Canadian Mineralogist
Vol. 15, pp. 135-161 (1977)

THE NUCLEATION AND GROWTH OF ALKALI FELDSPARS FROM HYDROUS MELTS

PHILIP M. FENN

Tuttle-Jahns Laboratory for Experimental Petrology and Department of Geology, Stanford University, Stanford, California 94305

ABSTRACT

Nucleation-density and approximate growth-rate data have been measured for eight bulk compositions in the system $NaAlSi_3O_8$-$KAlSi_3O_8$-H_2O at a confining pressure of 2.5 kbar. Melts containing from 1.7 to 9.5 wt. % H_2O were homogenized for 96 hours at 1000°C, then rapidly quenched to a temperature below the liquidus and held for a specified period. Significant lag times between the quench and the onset of internal nucleation are observed. Both the nucleation density and linear growth rate conform to the classical pattern, that is, both increase to a maximum then decrease as the temperature of the nucleation and growth stage is decreased. The nucleation-density curves typically peak at lower temperatures than the growth-rate curves. The maximum growth rates are observed for the H_2O-undersaturated melts and reach values of 5.2×10^{-6} cm/sec. The Na/K ratio of the initial melt has little influence on the kinetics or on the crystal morphology. The maximum observed growth rates and nucleation densities decrease and the positions of the maxima shift toward the liquidus as the initial H_2O content of the melt is increased. The variation of crystal morphology with temperature is nearly identical for all bulk compositions. Tabular, faceted crystals are the stable form within 40°C of the liquidus whereas a spherulitic morphology is dominant at lower temperatures. Applications of this type of high-temperature, high-pressure crystal growth in studies of trace and minor-element distributions phase equilibria, mineralogy, and textural development are discussed.

SOMMAIRE

La densité de nucléation et le taux de croissance approximatif de huit compositions dans le système $NaAlSi_3O_8$-$KAlSi_3O_8$-H_2O ont été mesurés à une pression ambiante de 2.5 kbar. Des charges d'une teneur pondérale de 1.7 à 9.5% H_2O ont été homogénéisées pendant 96 heures à une température de 1000°C, puis trempées rapidement à une température inférieure au liquidus, pendant un temps déterminé. D'importants écarts de temps entre la trempe et le début de la nucléation interne ont été observés. La densité de nucléation et le taux linéaire de croissance se conforment au modèle traditionnel: ils croissent jusqu'à une valeur maximale puis décroissent à mesure que la température de la nucléation et du stade de croissance diminue. De façon caractéristique, les courbes de la densité de nucléation atteignent des pics à des températures inférieures à celles du taux de croissance. Les taux maxima de croissance se rancontrent dans les charges sous-saturées en H_2O et atteignent 5.2×10^{-6} cm/sec. Le rapport Na/K de charge initiale a peu d'effet sur la cinétique ou sur la morphologie cristalline. A mesure que la teneur initiale en H_2O du bain augmente, les taux maxima de croissance et des densités de nucléation diminuent et leurs positions se rapprochent du liquidus. Les variations de morphologie cristalline avec la température, sont presqu'identiques pour toutes les compositions étudiées. A 40°C du liquidus, on trouve des cristaux tabulaires à facettes stables, tandis qu'une morphologie sphérolitique domine à des températures inférieures. Les applications de ce genre de croissance cristalline, à haute température

et haute pression, dans les études de distribution d'éléments mineurs et en traces, dans les équilibres de phase, en minéralogie et dans le développement de texture, sont discutées.

(Traduit par la Rédaction)

INTRODUCTION

The textures and fabrics exhibited by the common igneous rocks have been widely used by petrographers in outlining the crystallization sequence of the constituent minerals as well as the cooling history of the entire suite of rocks under investigation. Some of the earliest experimental studies of igneous processes (Hall 1798; Daubrée 1879; Fouqué & Michel-Lévy 1882; etc.) were concerned with the duplication of the textures of natural igneous rocks by melting and recrystallization from the melt. The success of these early experimentalists in not only synthesizing virtually all of the common rock-forming minerals, but also in elucidating the nature of the processes involved in the textural development of igneous rocks, led Iddings (1889) and other prominent petrographers of the day to express considerable optimism and to suggest further experimental studies, especially in granitic systems. Iddings stated the nature of the problem facing the experimentalist as follows:

> The results of experimentation are far from the solution of the problem before us. They have not yet succeeded in producing the minerals — quartz, orthoclase, mica, and hornblende — in the manner in which they occur either in volcanic rocks or in the coarsely crystalline ones; nor have they produced the feldspars in those isomorphous series so common to eruptive rocks. In this respect they have only suggested the possible necessity of a mineralizing agent, and have indicated the lines upon which further research should be made . . . (1889, pp. 94-95.)

In spite of the early success and promise of this type of experiment, the emphasis of experimental petrology shifted, almost totally, from the duplication of naturally occurring textures to the delineation and application of the equilibrium phase relations of geologically relevant systems.

Following the leadership of N. L. Bowen, experimental petrology concerned itself with the chemical and thermodynamic aspects of the crystallization process in igneous systems. Although extremely valuable from other viewpoints, these studies have failed to duplicate the more important textural features which are still the most widely used genetic indicators in the study of igneous rocks. After eighty years of careful experimentation, the criticisms expressed by Iddings are still valid.

It is a widely accepted fact that most igneous rocks have their origins as a silicate melt. Upon cooling, crystals of various oxide and silicate phases nucleate and grow at the expense of the melt until the mass is completely crystalline. Assume, for the purpose of the present argument, that the process is arrested at this point and the possible effects of autometamorphism, metasomatism, weathering, etc., are ignored. The task of the petrologist is to take this crystalline aggregate, an igneous rock, and by using its mineralogical makeup, bulk chemistry, texture, and fabric, deduce its past history and origin. He must predict and discuss the nature and effects of the various igneous processes which formed this rock when all that he has to work with is the end product of these processes. The tools with which he undertakes this task include a great deal of intuitive reasoning based upon his own careful observations and the observations of his predecessors, and a vast body of experimental data dealing with the behavior of rocks and minerals subjected to elevated temperatures and pressures. It is the application of this experimental data to natural rocks which must be considered at the present time.

Arguments based on the thermodynamic stability of the various phases in a rock have been used to determine the order of crystallization of these phases, yet as Miers & Issac (1907) have demonstrated experimentally, the process of nucleation can reverse such an order. Thermodynamic arguments also predict the temperature-pressure regime in which a certain mineral may stably grow from the melt but give no indication as to the ultimate size or morphology of the crystals. In fact, the thermodynamic stability of a mineral is a necessary but not sufficient condition to ensure its presence in the final product. As an example, phase-equilibrium data alone cannot effectively distinguish among a granite, an aplite, a pegmatite, or a rhyolite of similar bulk compositions. Much genetic information is contained in the kinetics and mechanisms of igneous processes, information which cannot be derived from phase-equilibrium studies. As long as textures are used in the interpretation of igneous petrogenesis, fundamental information on the processes involved in textural development is needed. Unfortunately, such information is not currently available for geologically significant systems.

Much of the problem lies in the reliance of the experimental petrologist on the attainment and demonstration of thermochemical equilibrium. Such an equilibrium state is, by its very definition, static, whereas the processes and reactions which are being modelled are dynamic. Phase-equilibrium data are extremely valuable in that they provide for the prediction of the

initial and final assemblages of a reaction or process as well as providing a means for bracketing the location of such a reaction or process in pressure-temperature space. The equilibrium data, however, provide little or no information about the mechanism, path, extent, or rate of the reaction or process. The two most basic, and most important, igneous processes are the nucleation of crystals and their subsequent growth from the melt.

The initiation of crystal growth from a homogeneous, undercooled melt requires the existence of a stable nucleus of sufficient size to stimulate further growth. How these nuclei are formed and at what rate they are formed are the bases of classical nucleation theory as put forth by Volmer & Weber (1925) and modified for condensed systems by Turnbull & Fisher (1949).

Once the nuclei have formed, crystal growth will occur spontaneously with a net reduction in the free energy of the system. The mechanisms and rate of the crystal-growth process and their effects upon the morphological development of the crystals are the subjects of an enormous body of literature. The most prominent crystal-growth theories and their application to experimental data are reviewed and ably discussed by Jackson *et al.* (1967), Tiller (1970), and Kirkpatrick (1975). Before these theories can be applied to common plutonic systems, basic kinetic data on the processes of nucleation and crystal growth in complex aluminosilicate compositions must be gathered; phase equilibrium data alone will not suffice.

Since 1925, there have been few detailed studies of nucleation and/or crystal growth in geologically relevant systems. Outstanding among these is the work of Winkler (1947) in which he reported quantitative nucleation and growth-rate data for nepheline grown from a melt in the system Na_2CO_3-Al_2O_3-SiO_2-LiF. The data were analyzed with regard to an explanation of the crystal size distributions observed in dykes. Unfortunately, the significance and impact of this study were lost within the plethora of phase equilibrium data being presented at that time.

Recently, there has been a resurgence of interest in kinetic processes among experimental petrologists. Lofgren (1974) has shown that the textures and chemical zoning patterns observed in natural plagioclase feldspars can be duplicated and studied in detail in the laboratory. Current interest in lunar and deep-sea basalts has generated several interesting experimental studies which focus upon nucleation and crystal growth from the melt and their relationship to textural development (Lofgren 1974; Lofgren *et al.* 1974; Walker *et al.* 1976; etc.) The work of Kirkpatrick (1974) on synthetic pyroxenes has demonstrated that accurate growth-rate data can be obtained in geologically important systems and analyzed in terms of gaining a better understanding of the mechanisms involved in the growth process. Kirkpatrick (1976a) also proposed that such kinetic data might be used in a predictive sense to estimate the growth rates for other phases without necessitating extensive experimentation. Swanson (1976) has studied the growth of alkali feldspar, plagioclase, and quartz from synthetic granite and granodiorite melts and discussed the development of textural features through the simultaneous crystallization of two or three phases. It seems that experimental petrology has come full circle from the 1880's through the 1970's with the processes involved in the crystallization of igneous rocks as the central theme and textural development as the vehicle for research.

This paper presents part of a continuing experimental study of the alkali feldspars within the system $NaAlSi_3O_8$-$KAlSi_3O_8$-H_2O at 2.5 kbar. Semi-quantitative kinetic data on the nucleation and growth rate of alkali feldspars from melts within the system will be described and analyzed with special emphasis on the role of H_2O. Preliminary results of this study were reported by Fenn (1972, 1974).

The System $NaAlSi_3O_8$-$KAlSi_3O_8$-H_2O

The alkali feldspars constitute one of the prominent modal fractions of the common granitic and syenitic plutonic rocks and their extrusive equivalents. Owing to this abundance, and to the wide variety of morphologies and textures which they exhibit, the alkali feldspars have been widely studied both in the field and laboratory. Properties such as grain size, spatial distribution in outcrop, morphology, bulk chemistry, structural state, and trace-element content have been extensively used as genetic indicators for various suites of rocks. Much of the experimental work of the past two decades has been focused on the phase relations of alkali feldspars, both as a separate mineral group and in conjunction with other components in the modelling of natural rock compositions. Because of their common occurrence in igneous rocks, the wide usage of their textural relations by petrographers, and their irrepressible popularity among experimentalists, mineralogists, and crystallographers, the alkali feldspars are an ideal mineral group on which to focus a study of nucleation and growth from silicate melts.

The bulk compositions of natural alkali feld-

spars lie on or very near the join $NaAlSi_3O_8$-$KAlSi_3O_8$. The phase relations along this join, which were described in detail by Schairer (1950), show an isomorphous series with a minimum on the liquidus modified only by the incongruent melting of potassium-rich compositions to leucite plus a SiO_2-rich melt. The end members, albite ($NaAlSi_3O_8$, hereafter abbreviated Ab), and potassium feldspar ($KAlSi_3O_8$, hereafter abbreviated Or without regard for its structural state), can be readily synthesized by a variety of techniques (Friedel & Sarasin 1883; Daubrée 1857; and numerous others) but are extremely difficult to crystallize directly from the melt. Day & Allen (1905) were not able to crystallize albitic plagioclase following the preparation of a melt; in fact, they reported extreme difficulty in even melting a sample of a relatively pure natural albite. Dietz *et al.* (1970) studied the superheating of albite and found that significant time is required to melt this feldspar at hyperliquidus temperatures. Crystallization proved to be even more difficult. Schairer & Bowen (1956) reported holding a sample of albite glass at approximately 100°C below its liquidus for a period of five years without observing any sign of crystallization. At the potassium end, the incongruent melting behavior of these compositions prohibits the direct synthesis of feldspars from the melt. Intermediate compositions have not been studied in detail, but is is expected that the difficulties observed in the melting and crystallization of albite would continue to these compositions.

The addition of mineralizers (fluxes) to the melt at elevated pressures, as suggested prior to 1889 (e.g. Iddings 1889), makes it possible to readily grow large crystals of these phases directly from the melt. Mustart (1969) has reported the growth of large (up to 2 mm) single crystals of both albite and potassium feldspar from melts fluxed with alkali disilicate-H_2O mixtures. Lofgren (1974) reported the growth of albite from melts fluxed with H_2O alone at a pressure of 5 kbar. At pressures exceeding approximately 2.6 kbar, the potassium feldspar melts congruently in the presence of excess H_2O (Goranson 1938), thus allowing for the possibility of growth from melts in the system $KAlSi_3O_8$-H_2O. The intermediate compositions of the alkali feldspar series, being of considerable interest to petrographers and petrologists, were selected for the present study of nucleation and growth of alkali feldspars from the melt.

Prior to studying a process such as nucleation or crystal growth, it is necessary to have a firm understanding of the equilibrium phase relations of the system being investigated. More specifically, the location and trend of the liquidus in temperature-composition space are vital. To this end, the equilibrium phase relations in the system Ab-Or-H_2O have been determined at a confining pressure of 2.5 kbar. This pressure was chosen for three basic reasons. First, there is an interval of approximately 50°C between the crest of the alkali feldspar solvus and the minimum on the solidus. This permits the growth of a continuous series of intermediate alkali feldspars in the subsolidus region. At higher pressures (in excess of 5 kbar), the solvus intersects the solidus and compositionally intermediate feldspars are unstable with respect to exsolution. Second, the pressure is high enough that the primary field of leucite is limited to a very small

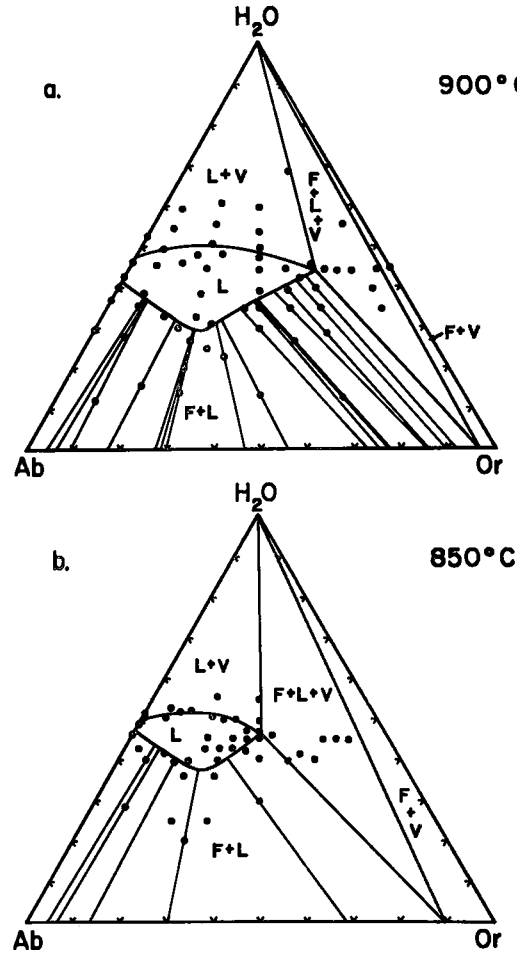

FIG. 1. Equilibrium isothermal sections for the system $NaAlSi_3O_8$-$KAlSi_3O_8$-H_2O at 2.5 kbar. All compositions are in mole percent. F = alkali feldspar, L = hydrous silicate liquid, V = free aqueous vapor.

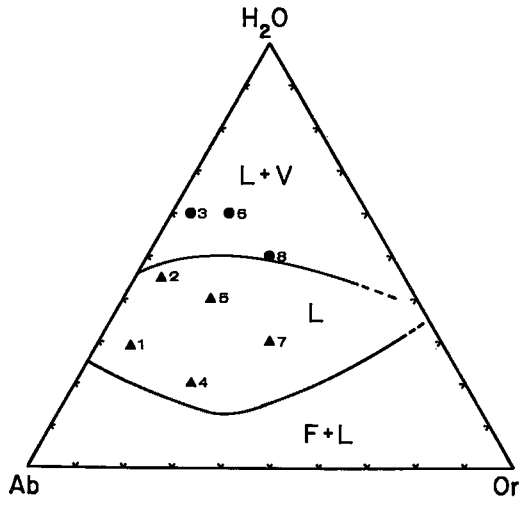

FIG. 2. Eight bulk compositions used in the present study plotted on 1000°C, 2.5 kbar equilibrium section. Compositions and phase designations as in Figure 1.

region around the potassium end member. Third, the pressure is low enough that it simulates the inferred depth of emplacement (8-9 km) of many of the continental granitic complexes, yet it is high enough that a wide range of hydrous melt compositions may be derived without necessitating unreasonable temperatures.

Two isobaric, isothermal sections which illustrate the general arrangement of the phase fields and their response to a change in temperature are presented in Figure 1. Details of the derivation and significance of these sections are not pertinent to the scope of the present paper and will be presented elsewhere. For the purpose of crystal-growth studies it is only necessary to note the location and rapid expansion with increasing temperature of the aqueous vapor-absent liquid field (*L*). The relative size of this field makes it possible to prepare homogeneous, single-phase melts over a wide range of both H_2O content and Na/K ratio without necessitating temperatures in excess of 1000°C. The eight bulk compositions selected for detailed nucleation and growth studies are presented in Figure 2 superimposed on the 1000°C isobaric section. Three anhydrous compositions (Or_{10}, Or_{30}, and Or_{50}) and specific H_2O contents for each were selected such that at 1000°C five of the bulk compositions consist of a homogeneous silicate liquid (melt) and the remaining three consist of a two-phase assemblage of silicate liquid plus a free aqueous vapor. These two groups of compositions are indicated on Figure 2 by triangles and circles respectively. Detailed descriptions of

TABLE 1. BULK COMPOSITIONS

NUMBER	ANHYOROUS COMPOSITION*	WT. % H_2O	MOLE % H_2O	$T_{LIQUIDUS}$ (°C)
1	Or_{10}	2.7	29	945
2	Or_{10}	5.4	45	840
3	Or_{10}	9.0	59	775
4	Or_{30}	1.7	20	970
5	Or_{30}	4.3	40	840
6	Or_{30}	9.5	61	765
7	Or_{50}	2.8	30	955
8	Or_{50}	6.2	50	815

*Mole percent $KAlSi_3O_8$

the eight bulk compositions are included in Table 1. This choice of compositions allows the evaluation of both of the chemical variables, H_2O content and Na/K ratio, as they affect the kinetics of nucleation and crystal growth and the morphology of the resultant crystals.

EXPERIMENTAL METHOD

The starting materials were prepared at 5 mole % intervals between $NaAlSi_3O_8$ and $KAlSi_3O_8$ using a coprecipitated gel technique modified after Luth & Ingamells (1965). The presence of 0.12 wt. % Na_2O (determined by flame photometry) in the Ludox (E. I. du Pont de Nemours) used as a source of SiO_2 was accounted for in the preparation of the gels with the exception of the potassium end member. The gels were ground to an average of less than 5 μm prior to loading into 2.0 mm O.D. platinum capsules which contained a known amount of distilled, de-ionized H_2O. All of the experiments reported in the present study were performed in an internally heated pressure vessel modified considerably from the design of Yoder (1950), using argon as the pressure medium. Inconel-sheathed Pt/Pt-10% Rh or Chromel/Alumel thermocouples, periodically calibrated against the melting points of sodium chloride and gold, were used for temperature measurement and control. Pressure was monitored using both a Heise gauge and a 120-ohm manganin coil in conjunction with a Carey-Foster bridge. The reported temperatures and pressures are thought to be accurate to within 10°C and 100 bars, respectively.

Electron microprobe studies were done on an ARL-EMX microprobe in the School of Earth Sciences at Stanford University. Accelerating potentials of 15 and 20 kV were used and the beam current was maintained at a low level to

prevent the volatilization of the alkalis, especially in the hydrous glasses. Beam currents on the order of 0.010 to 0.015 μA were found to have no observable effect on the sodium count rate from an albite glass containing 2.4 weight % H_2O. The standards employed in this part of the study were low-H_2O content (less than 2.5 wt. %) glasses synthesized at 1000°C and 2.5 kbar from the same gels used in the crystal-growth runs. These standards were independently checked against a natural adularia analyzed by the late Dr. C. O. Hutton and found to be good to within one weight % for each element. Spot analyses were made to check compositional homogeneity and beam scans were performed to check for chemical gradients at crystal-liquid interfaces.

X-ray powder diffraction patterns were obtained for several of the synthetic alkali feldspars. The patterns were measured from films taken on a Nonius Guinier-deWolff focusing camera using a fine-focus copper-anode tube. The camera was aligned such that no splitting of the Cu$K\alpha_1$-$K\alpha_2$ doublet was observed between 15 and 60 degrees 2θ. A spinel (a=8.0833Å) internal standard was employed and the accuracy of measurement of the individual peak positions is thought to be $\pm 0.010°$ 2θ or better. Unit-cell parameters for six alkali feldspars grown from the melt were obtained using the least-squares program of Evans *et al.* (1963). The fixed-index option was used and all peaks were assigned unit weight. These unit-cell parameters will be compared with those obtained by the same techniques from alkali feldspars synthesized directly from the gel under similar conditions of temperature and pressure.

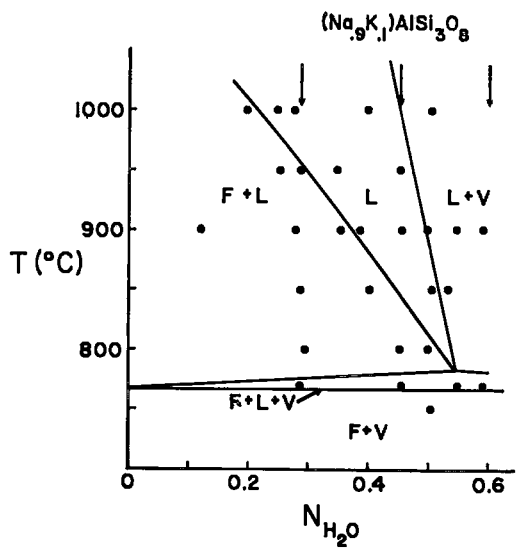

FIG. 3. Pseudobinary temperature-composition section for the system $(Na_{0.9}K_{0.1})AlSi_3O_8$-$H_2O$ at 2.5 kbar. All compositions in mole %, phase designations as in Figure 1; vertical arrows indicate compositions used in present study.

Two distinct experimental modes were employed. First, what will be referred to as the direct-synthesis approach was used to determine the equilibrium phase relations. In this method a set of capsules is taken from ambient conditions directly to the pressure and temperature conditions of the synthesis experiment, held for a specified period of time (long enough to achieve "equilibrium") and then quenched. Alkali feldspars formed using this approach crystallized from a finely divided gel and typically have an average grain size of 20 μm.

A second set of experiments using a different technique was performed to study the nucleation and growth phenomena. These experiments consisted of a homogenization period of 96 hours at 1000°C and 2.5 kbar, followed by a rapid, isobaric quench to a lower temperature at which nucleation and subsequent crystal growth occurred. In this method the alkali feldspars grew directly from an undercooled melt, a process much more akin to natural igneous processes than the synthesis from a gel as described previously.

The temperature interval between the temperature of the nucleation and growth step and the liquidus temperature for each bulk composition will be referred to as the undercooling in the following discussions. In order to clarify the exact nature of the nucleation and growth experiments, Figures 3-5 present the equilibrium pseudo-binary temperature-composition sections for the bulk compositions studied. The relative positions of the eight bulk compositions used in this study are indicated by the vertical arrows which terminate at 1000°C. This point indicates the state of the system during the homogenization period. Nucleation and growth were investigated at 50°C intervals from 950° to 500°C. At each isotherm no fewer than two separate experiments were carried out with typical nucleation and growth steps of 24 and 48 hours; however, steps as short as 6 hours and as long as 240 hours were used at specified isotherms. Two capsules of each bulk composition were placed in the pressure vessel for each experiment in which a feldspar was stable at the temperature of the nucleation and growth step. These duplicate capsules were placed in direct contact with one another for the duration of the entire experiment. Thus at each isotherm, each of the bulk compositions investigated was represented

by no fewer than four and occasionally by as many as eighteen distinct samples.

Upon completion of the nucleation and growth step, the experiment was rapidly quenched, again under isobaric conditions, to room temperature; the pressure was released and the samples removed from the pressure vessel. Each capsule was carefully opened and the entire charge immersed in oil. The number of nucleation sites (crystallization centers) was counted and the longest dimension of the crystals measured using a micrometer ocular on a standard petrographic microscope. For each bulk composition, one of the duplicate charges was selected and a thin section prepared.

Kinetic Measurements

Nucleation

Only those nucleation sites which could be shown to be completely enclosed in residual glass were included in the present measurements. These internal nucleation sites were distinguished from those heterogeneous sites at which nucleation occurred on the capsule walls, in the crimp at the end of the capsule, or on a pre-existing crystal surface. The term internal nucleation is used to describe these sites to avoid the problems and pitfalls inherent in the usage of the term homogeneous nucleation. In its strictest sense, homogeneous nucleation requires the formation of nuclei at random from a chemically and physically homogeneous melt. As the structural complexity and viscosity of the melt increase, the probability of true homogeneous nucleation ever occurring diminishes greatly. Brown & Ginell (1962), in discussing the reconstructive processes involved in the devitrification of glasses, concluded that "... in silicate glasses one can probably discount any likelihood of homogeneous nucleation ever occurring...". Thus the term internal nucleation is preferred for those sites which show no obvious relationship to a physical interface or foreign body within the melt.

The determination of a nucleation rate, that is, the number of nuclei formed per unit volume of melt in unit time, typically involves a two-step heat treatment with time and temperature carefully controlled. The first step is the nucleation step during which nuclei are formed within a fixed time interval from a sample of a homogeneous glass. The temperature of this step is commonly well below the liquidus for the composition being studied, often 200° to 300°C. Following this timed nucleation step the sample is heated to a significantly higher temperature at which the growth rate on these pre-formed nuclei is sufficiently fast to quickly develop them

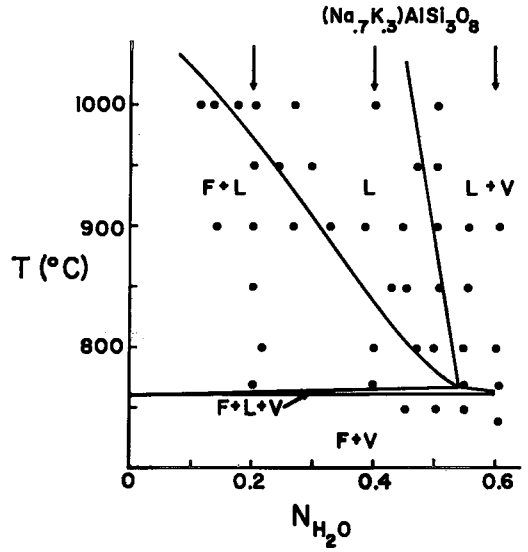

FIG. 4. Pseudobinary temperature-composition section for the system $(Na_{0.7}K_{0.3})AlSi_3O_8$-$H_2O$ at 2.5 kbar. All compositions in mole %, phase designations as in Figure 1; vertical arrows indicate compositions used in present study.

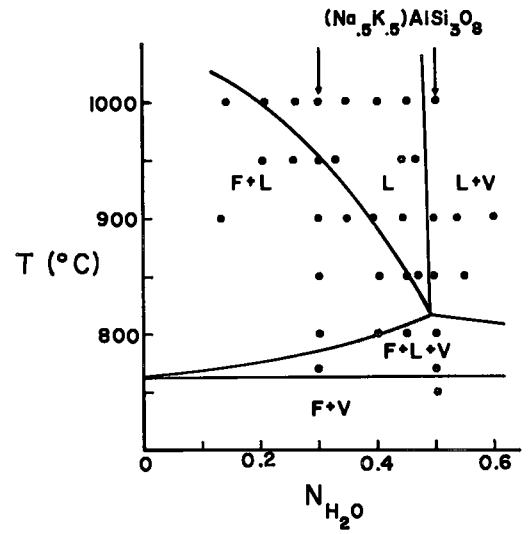

FIG. 5. Pseudobinary temperature-composition section for the system $(Na_{0.5}K_{0.5})AlSi_3O_8$-$H_2O$ at 2.5 kbar. All compositions in mole %, phase designations as in Figure 1; vertical arrows indicate compositions used in present study.

to an observable size. By making several experiments with different nucleation-step durations, a value for the nucleation rate can be determined. Such quantitative nucleation-rate measurements were not collected in the present study for two basic reasons. First, with regard to natural processes in the development of primary igneous textures, the time-temperature path followed by experiments, such as those just described, is extremely difficult to envisage. Second, significant periods of time between the initial quench to the nucleation and growth isotherm and the formation of the first nuclei were encountered in the alkali feldspar system. This lag time was often on the order of 24 to 72 hours and made it extremely difficult to establish a time frame for the measurement of a nucleation rate. In view of these difficulties, the only nucleation-related variable which could be measured from the present experiments was the nuclei density, that is, the number of nuclei formed per unit volume over the duration of the nucleation and growth step.

Nucleation incubation period

Turnbull (1948) has described and theoretically analyzed the time transient between the quench and the appearance of the first nucleus, a period which he referred to as the nucleation incubation period. It is a measure of the time necessary for a molecular system to re-establish its equilibrium cluster-size distribution following a sudden disruption such as a temperature quench. Until the clusters are able to grow to their new equilibrium sizes, the probability of thermal fluctuations in the melt being able to create a cluster of critical size is extremely small. In the present study, this incubation period manifested itself in the failure of certain experiments to show any sign of crystal growth after nucleation and growth steps of 72 hours or more. This was particularly true of experiments at very low or very high values of undercooling.

These incubation periods are not unique to this particular system. In his study of the nucleation and growth of nepheline from a LiF-fluxed melt, Winkler (1947) reported a period of 125 minutes between the quench and the first observable growth at an undercooling of 15°C. This period reduced steadily as the temperature of the experiment decreased; at an undercooling of 65°C only 6 minutes elapsed between the quench and the first appearance of crystals. Lofgren (1974) also reported problems in obtaining nucleation of plagioclase at low undercoolings. His data suggested that the length of the incubation period also varied with the composition of the melt. At an undercooling of approximately 40°C, An_{60} grew as tabular crystals up to 2 mm in length over a period of 24 hours whereas, at the same undercooling, An_{15} formed no nuclei after 144 hours. This presumably can be correlated with the increasing viscosity of the melt as the anorthite content decreases. Thus for the alkali feldspars, whose viscosities are significantly higher than the plagioclases, it is not surprising to find relatively long nucleation incubation periods.

If the exact duration of this nucleation incubation period were known, then accurate measurements of the nucleation rate might be made. One possible solution to this problem entails making several experiments at each isotherm and varying only the duration of the nucleation and growth step. Figure 6 represents an attempt to do this for two of the bulk compositions used in this study. By assuming a linear growth law for the experiments of 72 hours or less the intercept of the crystal size versus time line with the time axis should provide an accurate measure of the nucleation incubation period. The assumption of a linear growth law for the alkali feldspars is critical to this argument. Virtually all of the silicates which have been studied in detail show such a linear trend (cristobalite – Wagstaff 1968; nepheline – Winkler 1947; anorthite – Klein & Uhlmann 1974; calcic pyroxenes – Kirkpatrick 1974; and sodium disilicate – Meiling & Uhlmann 1967); thus, such a growth law would seem a reasonable assumption for the alkali feldspars, at least for short-duration experiments.

The intercepts on the abscissa of Figure 6 indicate nucleation incubation periods of 4 and 23 hours for Or_{10} + 2.7 wt. % H_2O and Or_{30} +

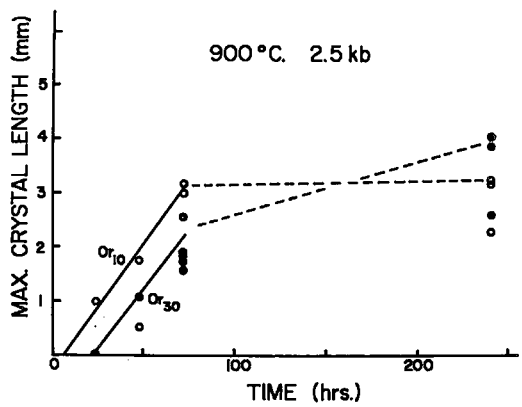

FIG. 6. Growth curves for two of the bulk compositions used in present study. Or_{10} + 2.7 wt. % H_2O (number 1) and Or_{30} + 1.7 wt. % H_2O (number 4).

1.7 wt. % H_2O respectively. At 900°C, the temperature of nucleation and growth, the undercoolings for these two bulk compositions are approximately 45°C for the first and 70°C for the second. These two incubation periods are also consistent with Lofgren's observations in the plagioclase feldspar system if the compositional effect he observed is indeed due to the increasing viscosity of the melt. The viscosity of hydrous silicate melts has been shown to be inversely related to the H_2O content; small additions of H_2O drastically decrease the viscosity (Shaw 1963; and others). In the dry system $NaAlSi_3O_8$-$KAlSi_3O_8$, Kani (1935) has shown that the viscosity of the melt increases as the potassium content increases. If these two observations are applied to the bulk compositions of Figure 6, the first (Or_{10} + 2.7 wt. % H_2O) should have the lowest viscosity and therefore the shortest incubation period — and in fact, it does.

Unfortunately, the extreme scatter of the raw data about the growth lines on Figure 6 indicates that these values of the nucleation incubation period are not of sufficient accuracy to permit a quantitative estimate of the exact time of the nucleation event. Further evidence of the inaccuracy of this estimate comes from experiments which are not plotted on Figure 6, but which were done at 900°C. In comparing the duplicate samples from a particular experiment, it was all too frequently found that one of the charges had nucleated and grown alkali feldspars, but its twin showed no sign of nucleation. It is apparent from this and from the observations reported above, that nucleation in this system is inhibited not only by the incubation period but also by the probabilistic nature of the nucleation event itself. Since the data presented on Figure 6 represent 38 days of experimentation and the value of the conclusions is questionable, this type of exercise was not carried out for each of the other nine isotherms investigated during this study.

FIG. 7. Photomicrographs of experiments on bulk composition 1 (Or_{10} + 2.7 wt. % H_2O) at 2.5 kbar. The white scale bar is equivalent to 1 mm. Crossed polarizers.
a) Nucleation and growth at 900°C, 72 hrs., ΔT = 45°C.
b) 850°C, 24 hrs., ΔT = 95°C.
c) 800°C, 24 hrs., ΔT=145°C.
d) 740°C, 48 hrs., ΔT=205°C.

Crystal growth rate

Growth rates were calculated by dividing the maximum length of internally nucleated crystals by the duration of the entire nucleation and growth step. This type of approximate calculation was necessitated by the nucleation problems discussed previously. The variability of the nucleation incubation period, when coupled with the necessity of enclosing the samples in noble-metal capsules to retain the volatile component (thereby eliminating the direct observation of the onset of nucleation and growth), makes the determination of the exact time over which the growth took place impossible. Consequently, the duration of crystal growth was assumed to be equivalent to the length of the nucleation and growth step. This assumes that the nucleation was spontaneous upon quenching (obviously not true in most instances), but in view of the problems indicated above, it is the only consistent way to treat all of the data for the ten isotherms. Therefore, all of the growth rate data reported are minimum values; the true growth rates could be significantly higher if the duration of the nucleation incubation period were excluded from the time used in the calculation.

Although the general technique of measuring a crystal and dividing by a fixed time interval seems simple and straightforward, it is not without its own problems. To illustrate the nature of these problems, Figures 7 and 8 show a series of products from bulk composition 1 on Figure 2 (Or_{10} + 2.7 wt. % H_2O) arranged in order of decreasing temperature of growth. Some of the problems involved in the accurate measurement of growth rates are graphically illustrated in these photomicrographs. In Figure 7a, b, and c, many of the crystals are truncated by the capsule walls; this is a problem in using such a small sample (roughly 30 mg of material in a 2 mm O.D. capsule). Fortunately, in each charge a few of the crystals were oriented nearly parallel to the long axis of the capsule and were evidently able to grow unobstructed by physical barriers. In Figure 7d, the number of nucleation sites has increased to the point where crystal growth is obstructed by mutual interference of crystals from different centers. The eventual length of any of these crystals, had they been able to grow freely, is impossible to ascertain from this intergrowth. This problem becomes even more serious as the undercooling increases, as is evident from the charges pictured in Figure 8a, b.

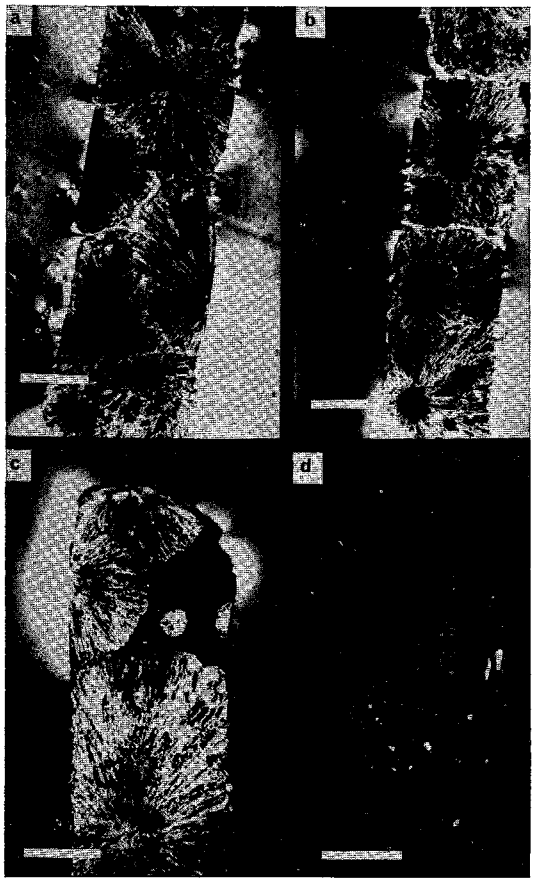

FIG. 8. Photomicrographs of experiments on bulk composition 1 (Or_{10}+2.7 wt. % H_2O) at 2.5 kbar. The white scale bar is equivalent to 1 mm. Crossed polarizers.
a) Nucleation and growth at 700°C, 24 hrs., ΔT =245°C.
b) 650°C, 48 hrs., ΔT=295°C.
c) 600°C, 48 hrs., ΔT=345°C.
d) 550°C, 48 hrs., ΔT=395°C.

The data plotted on Figure 6 demonstrate another type of problem which affects the hypersolidus experiments and which is independent of sample size. This is the problem of the establishment of crystal-liquid equilibrium. If a crystal growing from a melt held at 900°C is considered, it can be seen from Figure 6 that at some time between 72 and 240 hours, there must be a sharp decrease in the observed growth rate. At this temperature, the bulk compositions under consideration (1 and 3 from Fig. 2) lie in the feldspar plus silicate liquid field (see Fig. 3 or 4) and thus have associated with them an equilibrium two-phase tie-line such as those illustrated on Figure 1a. These tie-lines give not only the compositions of the two coexisting phases, but also the relative amounts at equilibrium. As crystal growth proceeds and this ratio of phases is approached, the growth rate must decrease until it is equal to zero at equilibrium. Whether the growth rate drops discontinuously to zero at this point or approaches it asymptotically cannot be determined from the present data. The significance of this decrease in growth rate can be seen from a plot such as Figure 6. If only one nucleation and growth experiment had been performed with a step duration greater than 72 hours, the observed growth rate would be considerably lower than that derived from the shorter experiments.

The problems involved in the formation of nuclei make it difficult to establish the beginning of the growth period, and the problems of crystal obstruction or equilibrium make it difficult to fix the end. Thus the entire nucleation and growth period must be used in the calculation of growth rates which are by necessity minimum values, the true values being masked by the experimental difficulties. These problems illustrate the need for at least two separate experiments at each isotherm and for using the maximum observed growth rate from all of the experiments done at an isotherm as the characteristic value for that isotherm.

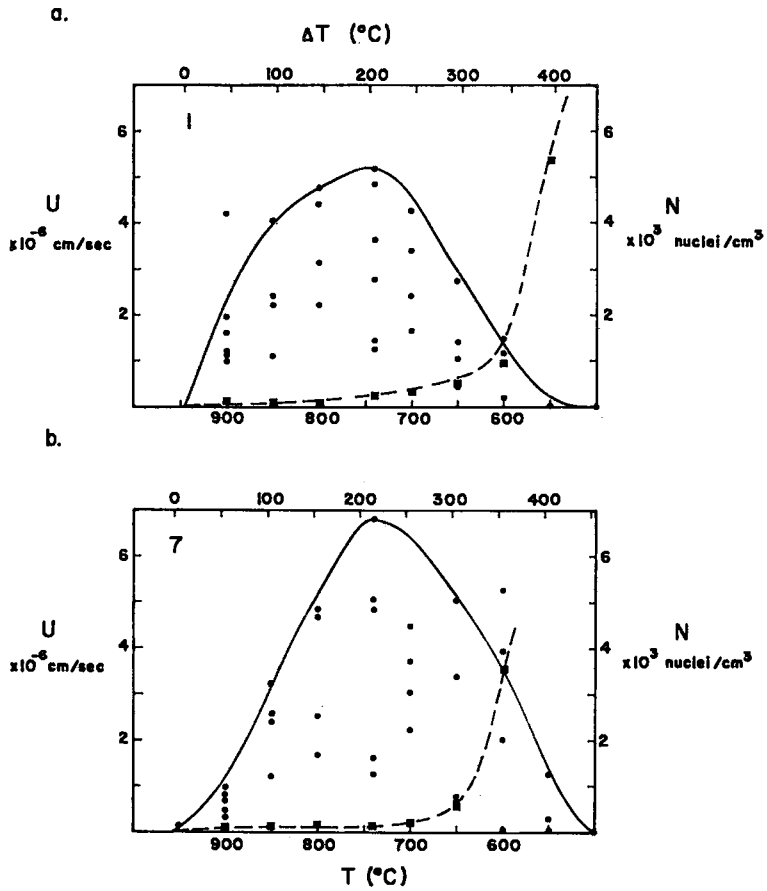

FIG. 9. Compilations of nucleation-density (N) and growth-rate (U) data for two bulk compositions; (a): Or_{10} + 2.7 wt. % H_2O (number 1); (b): Or_{50} + 2.8 wt. % H_2O (number 7). Solid circles are individual growth-rate measurements; solid squares are maximum observed internal-nucleation densities.

COMPILATION OF KINETIC DATA

Despite the myriad of problems involved in the measurements, definite patterns are observed when all of the data are assembled. Figure 9 represents a compilation of all of the data for two of the bulk compositions from Figure 2 (numbers 1 and 7). Only the maximum nucleation-density values are plotted, but all of the observed growth-rate data for each composition are included in the plots. The extreme scatter in the growth-rate data arises from the nucleation problems discussed previously. The solid curves shown on the Figure are drawn to enclose all of the growth-rate data from internally nucleated crystals and represent the best estimate of the general trend of the growth rate if nucleation is assumed to be spontaneous. One consequence of this assumption can be seen from those points lying above the growth-rate curves on Figure 9. These points, one at 900°C in Figure 9a and two at 600°C in Figure 9b, represent growth rates calculated from crystals which nucleated heterogeneously on the capsule walls at some time prior to the onset of internal nucleation. Had internal nucleation been spontaneous, the growth-rate curve would have shifted upward to the position of these points, if not higher. Since the nucleation problems were most serious at the lower and higher values of the undercooling, the true growth-rate curve would probably be more flat-topped than it appears in the Figure, but the relative position of the maximum should not shift appreciably.

The nucleation-density curves (dashed lines) for these two bulk compositions have not reached their maximum values within the temperature range of the experiments performed. The cal-

culated densities for 500°C in Figure 9a and 550°C in Figure 9b are beyond the range of the indicated scale. Had experiments been done at isotherms below 500°C, the nucleation curves would be expected to reach a maximum at some value of the undercooling and then decrease as the undercooling increased further. This type of behavior was observed in the other bulk compositions which had higher initial H_2O contents and is typical of other silicate systems which have been studied in detail (see for example Winkler 1947; or Rogers 1970). The effect of H_2O content on nucleation and growth will be discussed in a later section of this paper.

Discussion

Crystal morphology

Petrographic examination of numerous thin sections and oil mounts of the experimental charges revealed that virtually all of the crystals exhibit a characteristic preferred elongation. In all instances the crystals are length fast, indicating that they are elongate parallel or nearly parallel to the *X* optic axis. In the high-temperature alkali feldspar series, $a\Lambda X$ is 5 to 9°. To test the exact direction of elongation, several crystals were mounted for precession camera studies with their elongation axis parallel to the camera's spindle axis. On an (*h*0*l*) orientation photograph (unfiltered Mo radiation), the spindle axis is inclined approximately 26° to the (*h*00) streak and is perpendicular to the (00*l*) streak, thus indicating that the elongation axis is *a*. This is a common elongation direction of natural prismatic alkali feldspars (Iddings 1909) and one of the primary elongation directions of alkali feldspars in spherulitic intergrowths found in devitrified obsidian (Iddings 1891). In the first hydrothermal synthesis of albite, Friedel & Sarasin (1883) reported needles or tablets elongate parallel to the intersection of (001) and (010), which is identical to the habit displayed by the sodic alkali feldspars grown in the present study. The plagioclase feldspars also show similar habits. In an optical study of the plagioclases grown from melts by Day & Allen (1905), Iddings (1905) stated that the most common growth form was spherulitic aggregates of bladed crystals elongate along *a*. The plagioclase phenocrysts of lunar mare basalts also show *a*-axis elongation (Crawford 1973). The only variant to this seemingly general pattern is the anorthite crystallized from a glass by Klein & Uhlmann (1974), which they reported as being elongate along *c*.

The preferred growth of alkali feldspars and plagioclase along specific crystallographic directions is undoubtedly a reflection of structural controls. The concept of internal structure controlling external morphology is by no means new, in fact it is at the foundations of modern crystallography. For a discussion of the concept and its application to several crystal structures, see Dowty (1976). The application of these ideas to the growth of alkali feldspars from the melt is being investigated and will be reported on later.

The preferred growth along *a* was accompanied by another general orientation observed in the alkali feldspars grown during this study. In most of the charges, the crystals were found to lie with (010) parallel to the flattened sides of the capsule. This plane also corresponds to the plane of the thin sections pictured in Figure 7. The exact reason for this preferred orientation is not known, but may be due to some non-uniformity in the pressure distribution within the capsules (a very disturbing thought). In this orientation, the crystals can be seen to be bounded by {001} and terminated by pinacoid faces {$\bar{2}$01}, {100}, and rarely {$\bar{1}$01}. Based on these orientation data, the relative growth rates along the crystallographic directions of alkali feldspars can be established as $a>c>b$. It must be emphasized that all of the growth-rate data reported in this paper are for growth in the *a* direction.

The marked anisotropy in the growth rates along the crystallographic directions and the predominant radial habit of the crystal aggregates as illustrated in Figures 7 and 8 are characteristic features of spherulitic growth. Many of the crystal aggregates also show the characteristic extinction cross (Fig. 7d) and non-crystallographic low-angle branching. The hydrous alkali feldspar melt is an ideal medium for the growth of spherulites (Keith & Padden 1963). It is a high-viscosity melt, the growth rates are relatively slow, and over most of the range of undercooling investigated, the number of nuclei formed is low. The spherulites developed at lower undercoolings are, in the terminology used by Lofgren (1974), coarse and open (Fig. 7). As the undercooling increases, the individual crystal width decreases as does the spacing between adjacent crystals, resulting in the development of the fine, closed spherulites shown in Figures 8a and b. At still higher undercoolings, a change in this pattern is noticed. In Figure 8c, the crystal width appears to have increased, although this may be due to a dense packing of very fine fibrous crystals, and a prominent faceting at the terminations of the crystals can be seen. There

is also a significant amount of residual glass in this charge, whereas the two preceding charges (Fig. 8a, b) are virtually completely crystalline. This change is even more apparent as the undercooling is increased further. The charges pictured in Figure 8b, c, and d, are the same bulk composition and the duration of the experiments is identical; only the temperature of the nucleation and growth step is different. Instead of the smooth progression in morphology which was observed in the charges from Figure 7a through Figure 8b, there is a large disparity in both the number of crystallization centers and the apparent growth rate between the charge pictured in Figure 8d and any of the others. This may reflect a change in the nature of the medium from which the crystals grew.

Using the "two-thirds rule" as a relation between the liquidus temperature and the glass-transition temperature (Sakka & Mackenzie 1971), the glass transition for this particular bulk composition should occur at approximately 630°C. Considering the empirical nature of this "rule", although it does seem to work well for the dry alkali feldspar system (Vergano *et al.* 1967), and the dependence of the glass-transition temperature upon the cooling rate (Jones 1971), it seems possible that the glass transition for this bulk composition may lie very near the temperature of the experiment pictured in Figure 8c (600°C). Thus the crystallization of the charge pictured in Figure 8d may have taken place from a true glass rather than from a supercooled liquid as would be the case for the charges of Figures 7 and 8a, b.

The spherulitic growth forms shown in Figures 7 and 8 are typical of the growth of alkali feldspars from the three lowest-H_2O liquids (1, 4, and 7 on Fig. 2). The isolated tabular crystals observed at low undercoolings in the plagioclase feldspars by Lofgren (1974) were not observed at undercoolings as low as 45°C. Only one set of experiments on bulk composition 4 at 950°C (an undercooling of 20°C) showed any development of tabular crystals. The skeletal and dendritic crystal forms described by Lofgren were not found in any of the experiments on these low-H_2O compositions. For these compositions the variation of crystal morphology with undercooling is quite simple: isolated tabular crystals are stable at the very lowest undercoolings; coarse, open spherulites become stable at intermediate undercoolings; and finally the fine, closed spherulites are the stable form at the highest undercoolings investigated. This trend was observed by Lofgren (1974) for the albitic plagioclase in the presence of excess H_2O, although his data indicate the existence of tabular crystals of albite at undercoolings of up to 250°C; these would presumably be followed by spherulitic forms at greater undercoolings. The difference in the H_2O contents or in the viscosity of the melt may make a difference in the stability range of the different crystal forms.

As the initial H_2O content of the alkali feldspar liquid is increased, the morphological development follows the same general trend. Figure 10 illustrates a series of experiments on bulk composition 2 from Figure 2 (Or_{10} + 5.4 wt. % H_2O). The crystal forms shown (Fig. 10) are also typical of those found in experiments on the other intermediate-H_2O bulk composition (number 5 from Fig. 2). Again, isolated tabular crystals were not found at undercoolings as low as

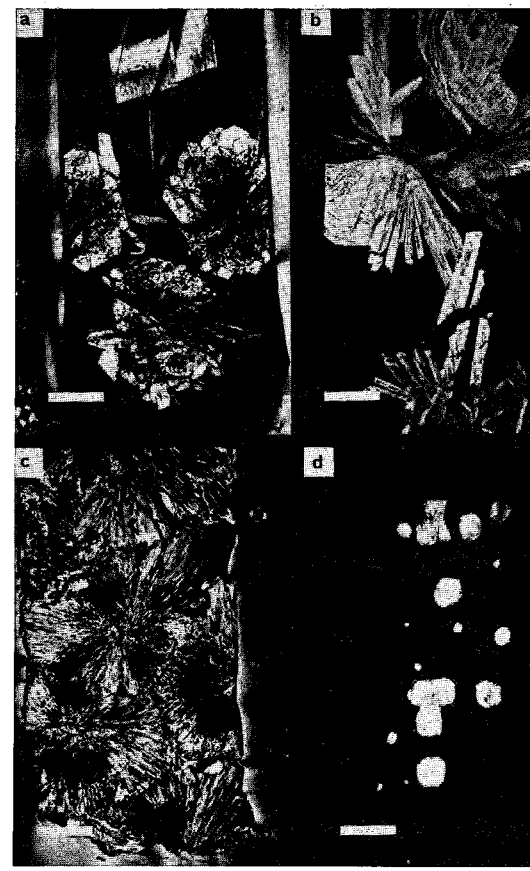

FIG. 10. Photomicrographs of experiments on bulk composition 2 (Or_{10} + 5.4 wt. % H_2O) at 2.5 kbar. The white scale bar is equivalent to 0.5 mm. Crossed polarizers.

a) Nucleation and growth at 800°C, 48 hrs., ΔT =40°C.
b) 740°C, 24 hrs., ΔT=100°C.
c) 650°C, 24 hrs., ΔT=190°C.
d) 550°C, 24 hrs., ΔT=290°C.

40°C (Fig. 10a) and the dominant growth form is spherulitic. At the lowest undercoolings investigated, the crystals are elongate on *a*, predominantly faceted, and show radial symmetry about the crystallization center. These bulk compositions show a somewhat less marked anisotropy in the growth rates along *a* and *c*, resulting in blocky crystals such as those shown in Figure 10a, b.

These particular bulk compositions also show another feature which was not observed in those with the lowest H_2O contents. The crystals in Figure 10b, especially those to the left of center in the photograph, are skeletal in that their cores contain areas of residual glass. These crystals apparently formed as open dendritic arrays, elongate on *a*, which were later filled in and faceted as shown in the photomicrograph. It is possible that this later growth occurred after the liquid had become saturated with H_2O. These compositions, although undersaturated during the homogenization step, are close to the saturation level at the temperatures of nucleation and crystal growth. Consider the equilibrium phase relations for this bulk composition as shown in Figure 3. The liquidus for this particular composition (45 mole % H_2O) is at approximately 840°C, and thus the first experiments in the present study which could have grown alkali feldspars would be those with a nucleation and growth step of 800°C. At this temperature, the crystals would coexist with an H_2O-undersaturated liquid, as do the crystals pictured in Figure 10. At the next lower nucleation and growth step, 740°C, the stable assemblage is a feldspar plus an aqueous vapor phase (the subsolidus assemblage) and the silicate liquid is thermodynamically unstable. The initial growth in such a situation may be a very rapid growth of dendritic feldspars from an H_2O-undersaturated liquid. Since the feldspars are anhydrous, H_2O must be concentrated in the residual liquid where it will eventually exceed the saturation level, and a separate aqueous vapor phase is evolved. Note from Figure 3 that, as the liquid is enriched in H_2O, its liquidus temperature decreases, and, consequently, the effective undercooling of the system also decreases. Thus the later growth on the dendritic arrays may take place at an undercooling where a tabular morphology is stable. Such tabular growth on a substrate of pre-existing dendritic crystals would lead to the formation of faceted crystals which may show the incomplete, skeletal forms displayed in Figure 10b. These compositional effects make it very difficult to interpret growth morphology from H_2O-undersaturated experiments when the growth takes place at temperatures between the liquidus and slightly below the solidus. The facets observed on most of the crystals grown under these conditions may have formed in response to these chemical effects and may not be indicative of the stable growth form. The same is true of the experimental charges pictured in Figures 7 and 8.

At higher undercoolings, compact spherulites are the dominant growth form from these intermediate-H_2O liquids; these forms are shown in Figures 10c and d. The crystals shown in Figure 10c are fibrous on a fine scale but appear to coalesce to form larger single crystals. This process may be very important in the development of igneous textures; the spherulitic aggregates might recrystallize into single prismatic crystals during the subsolidus cooling history of a plutonic igneous body. Such subsolidus recrystallization may explain why the growth forms of the alkali feldspars synthesized during the present study are not commonly observed in rocks from plutonic environments. This process is currently being investigated with synthetic material of granitic composition.

Again for this bulk composition there is a prominent break in the morphological trend at the highest undercoolings studied. The calculated glass-transition temperature for this composition is approximately 560°C, which would place the transition between the experiments shown in Figures 10c and d. This would mean that the charge pictured in Figure 10d crystallized from a glass, whereas the others crystallized from supercooled liquids. From these examples and the experience of others, it can be concluded that H_2O-undersaturated alkali feldspar liquids are good glass-formers, and that once the glass has formed, the rate of crystal growth diminishes rapidly. It is interesting to note that for the lowest H_2O contents, the nucleation density does not reach its maximum values until below the glass-transition; in the intermediate-H_2O experiments, the maximum nucleation density is near the glass-transition temperature. These observations may be significant in the development of fine-grained equigranular textures as is considered in a later section.

The growth morphologies of the H_2O-undersaturated experiments have been shown to be similar. There is a general progression from isolated tabular crystals at undercoolings less than 40°C to spherulitic aggregates which become less coarse and more closed as the undercooling increases. Only the appearance of skeletal crystals in the experiments with intermediate-H_2O content separates them from the others; it is possible that this may only be a reflection of the variation in the effective undercooling caused

by the redistribution of H_2O. To test the effectiveness of this compositional lowering of the undercooling in changing growth morphology, experiments were performed on three H_2O-oversaturated bulk compositions in which this effect would be minimized.

From the phase relations shown in Figure 1, it can be seen that, for any bulk composition in the liquid plus aqueous vapor field, the liquidus is defined by the passage of the leading edge (*L-V* edge) of the three-phase triangle ($F+L+V$) through the bulk composition as the temperature decreases. On a diagram such as Figure 1, which is plotted in molar ratios, the vapor composition is nearly pure H_2O (99+ % H_2O from the data presented by Luth & Tuttle 1969) and thus the *L-V* edge of the three-phase triangle would radiate from the H_2O apex. Therefore, bulk compositions with equivalent Na/K ratios would have identical liquidus temperatures if they were in the liquid plus aqueous vapor field. This is graphically shown in Figure 1a. Two points are plotted in the *L-V* field very near the leading edge of the three-phase triangle; even though their H_2O contents are quite different (45 versus 70 mole % H_2O), their liquidus temperatures would be virtually identical (slightly below 900°C). As a result, the concentration of H_2O in the residual assemblage during crystal growth from a liquid plus aqueous vapor assemblage will not create a lowering of the effective undercooling. The growth morphology of crystals grown from these H_2O-oversaturated assemblages should not be modified by any compositional effects, and the crystals should preserve their initial growth morphology.

The photomicrographs of Figure 11 represent a series of experiments on bulk composition 8 from Figure 2 (Or_{50} + 6.2 wt. % H_2O). This composition was oversaturated with respect to H_2O and growth occurred from a two-phase assemblage of liquid plus aqueous vapor. Figure 11a shows a single tabular crystal grown at 800°C (an undercooling of 15°C). The crystal is bounded by {001}, terminated by {$\bar{2}$01} and {100} (upper right), and contains trains of bubbles and glass inclusions which appear to decorate the advancing growth faces. Note that toward the center of the crystal these inclusions are parallel to {$\bar{2}$01} alone, but as the crystal grew further inclusions parallel to {100} were developed. This graphically illustrates the principle of the slower growing faces becoming dominant as growth proceeds. The distribution of these inclusions within the crystal is somewhat disturbing; their concentration toward the extremities of the crystal may suggest that the growth rate was not linear with time, or it may

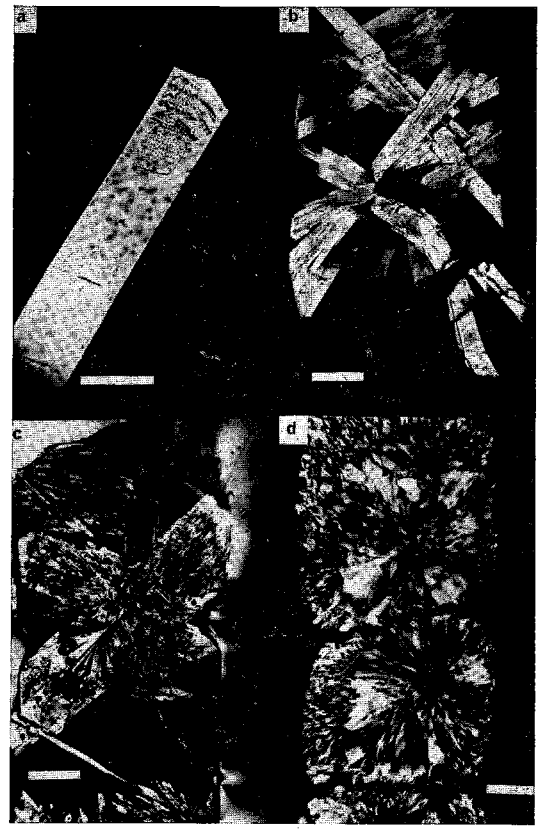

FIG. 11. Photomicrographs of experiments on bulk composition 8 (Or_{50}+6.2 wt. % H_2O) at 2.5 kbar. Crossed polarizers.

a) Nucleation and growth at 800°C, 48 hrs., ΔT =15°C; white scale bar = 0.25 mm.
b) 740°C, 24 hrs., ΔT=75°C; scale bar = 0.5 mm.
c) 700°C, 8 hrs., ΔT=115°C; scale bar = 0.5 mm.
d) 500°C, 72 hrs., ΔT=315°C; scale bar = 0.5 mm.

be that the inclusions near the center of the crystal have had sufficient time to crystallize or migrate out of the crystal. The crystallization of glassy inclusions is possible in this system since the compositions of the liquid and crystal are very similar, and alkali exchange and homogenization are rapid.

Another H_2O-oversaturated bulk composition (number 3) was crystallized at 740°C (an initial undercooling of 35°C) and found to produce similar isolated tabular crystals. Figure 11b shows a radial aggregate of acicular crystals, all elongate on *a*, from an experiment on bulk composition 8 at an undercooling of 75°C. Thus it appears that the tabular morphology is again

limited to a range of undercoolings of at least 35°C, but less than 75°C, for growth from liquid plus aqueous vapor assemblages. This is consistent with the previous observations on H_2O-undersaturated alkali feldspar compositions, but is a significantly narrower interval than that observed by Lofgren (1974) in the plagioclase feldspar system.

As the undercooling is increased for these H_2O-oversaturated compositions, the spherulitic morphology becomes predominant (Fig. 11c). Here the crystals are still rather coarse, but the radial arrangement, the uniform crystallographic orientation, and the excellent example of low-angle branching exhibited to the right of center in the photograph are distinctive of spherulitic growth. At the maximum undercoolings investigated in these compositions, a dramatic change in growth morphology is noticed. In the H_2O-undersaturated compositions, experiments below the glass-transition typically display an increase in the nucleation density and a drastic decrease in the observed growth rate; significant amounts of residual glass are present even after periods of 240 hours in the subsolidus region. The H_2O-oversaturated compositions, in contrast, were virtually completely crystalline and showed a strange feathery morphology as seen in Figure 11d. For this particular bulk composition, the calculated glass-transition temperature is approximately 543°C, which is above the temperature of the experiment which produced the charge in Figure 11d. Not only do the charges show this feathery morphology, but there appears to be a major change in the growth habit at the borders of the spherulites after roughly three-quarters of the charge is crystalline. This feature was observed in all of the H_2O-oversaturated experiments at the highest undercoolings, and may represent rapid growth on the quench. It appears that the effect of excess H_2O reduces the glass-forming ability of alkali feldspar liquids and causes very rapid imperfect growth at high undercoolings. This is the only significant variation in the general pattern of morphologies observed in all of the bulk compositions studied and represents an interesting area for further study.

To summarize, alkali feldspars grown from hydrous liquids in the system $NaAlSi_3O_8$-$KAlSi_3O_8$-H_2O display a consistent morphological pattern as the undercooling is increased. At low undercoolings, less than approximately 40°C, the stable growth morphology is the isolated tabular crystal. This gives way to spherulitic morphology with only minor appearances of skeletal or dendritic crystals as the undercooling increases. The pattern is similar to that observed by Lofgren (1974) but seems to be somewhat simpler in the relative unimportance of the skeletal and dendritic morphologies. This may be due in part to the chemical differences involved in crystallization from the two systems. The alkali feldspar liquid compositions used in the present study and their crystalline analogues are chemically similar; the aluminosilicate basis is not changed during the crystallization process, only the alkalis and H_2O must be redistributed over relatively long distances. In the plagioclase feldspars, Si and Al must be moved about in a coupled substitution with Na and Ca respectively. The necessity of varying the Si/Al ratio in the aluminosilicate framework of both the crystal and the liquid may be responsible for the development of a diffusion layer at the crystal-liquid interface of sufficient dimension to stabilize the dendritic and skeletal morphologies relative to the spherulitic (see discussion in Lofgren).

The role of the H_2O content of the liquid in influencing the growth morphology is not clear.

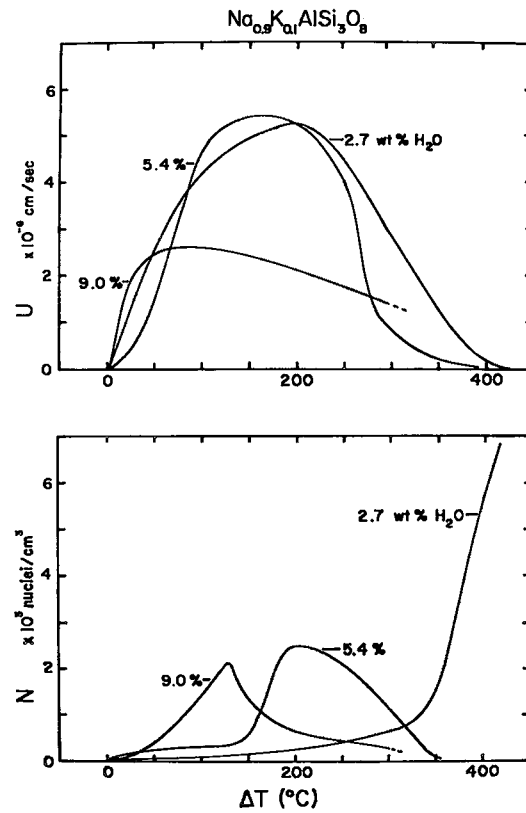

FIG. 12. Compilation of all nucleation density (N) and growth-rate (U) data for $(Na_{0.9}K_{0.1})AlSi_3O_8$ plus indicated H_2O contents. Plotted against system undercooling (ΔT).

The content seems to have a drastic effect on highly undercooled systems but at moderate to low undercoolings its effect is not discernible from the present data. Experiments are underway to specifically isolate and evaluate the role of H_2O in the chemically simpler system $NaAlSi_3O_8$-H_2O.

Effect of H_2O on kinetics

Aside from the effects of the H_2O content of the liquid upon crystal morphology as mentioned above, there is a far more dramatic effect on the nucleation density and crystal growth rate. Figures 12, 13, and 14 present a compilation of all of the nucleation and growth data gathered during the present study. The raw data have been omitted for the sake of clarity and the curves have been grouped according to the anhydrous compositions to display the effects of the H_2O content and Na/K ratio. Also, the nucleation-density and growth-rate data have been separated on each Figure.

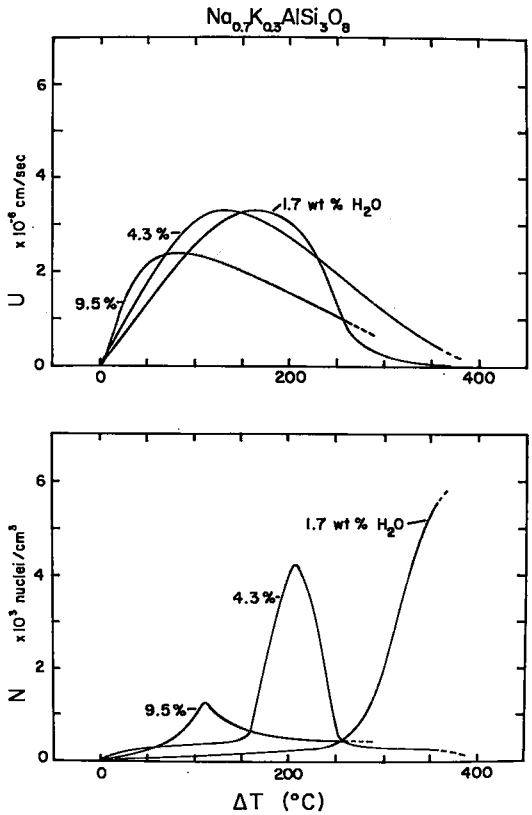

FIG. 13. Compilation of all nucleation density (N) and growth-rate (U) data for $(Na_{0.7}K_{0.3})AlSi_3O_8$ plus indicated H_2O contents. Plotted against system undercooling (ΔT).

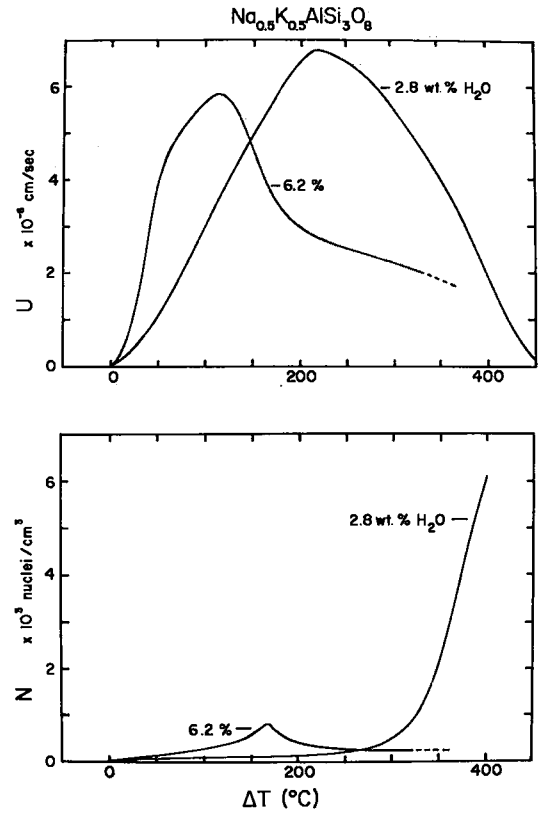

FIG. 14. Compilation of all nucleation-density (N) and growth-rate (N) data for $(Na_{0.5}K_{0.5})AlSi_3O_8$ plus indicated H_2O contents. Plotted against system undercooling (ΔT).

The nucleation-density curves for all three anhydrous bulk compositions show a striking and consistent pattern with increasing H_2O content. The maximum in the observed nucleation-density curves shifts almost linearly toward the liquidus as the H_2O content of the initial bulk composition increases. The absolute magnitude of this nucleation-density maximum also decreases markedly with increasing H_2O. The crystal growth-rate data also show similar trends, although not as dramatically as the nucleation-density data. There is a definite shift of the maxima toward the liquidus temperature, but the decrease in absolute magnitude is not as prominent. The decreases that are observed are not linear with H_2O content, as in the nucleation data, but are rather constant for the H_2O-undersaturated compositions and decrease as the systems become oversaturated. This decrease in growth rate as the H_2O saturation level is breached is contrary to the beliefs expressed by Jahns & Burnham

(1958) and others who felt that the presence of an aqueous vapor should enhance the crystal growth rate. Similar observations on the effect of excess H_2O on nucleation and growth were reported by Swanson (1976) for alkali feldspars, plagioclases, and quartz crystallized from a synthetic granodiorite liquid at 8 kbar. Lofgren (1973) also reported a reduction in the apparent growth rates of plagioclases grown from hydrous liquids as the H_2O content was increased.

The reasons for these dramatic changes in the nucleation density and growth rate as the H_2O content of the system is increased are not understood at the present time. Since there do not seem to be corresponding variations in growth morphology, it can be hypothesized that it is not the mechanism of the growth process that is being affected, but rather the rates of material transport and the reconstructive processes involved in nucleation and growth. At the heart of the problem is the interaction of H_2O with the silicate liquid; the exact nature of the chemical and physical interaction is at present still in the realm of speculation. A discussion of what is known of the role of H_2O in silicate liquids and its possible application to crystal growth is beyond the scope of the present paper. Experiments are being designed which should allow the collection of more accurate growth-rate data with which some of the problems mentioned above might be attacked. In spite of the lack of profound conclusions as to their origin, the trends observed in Figures 12, 13, and 14 are important to a discussion of the origin of igneous textutres, as will be discussed shortly.

The effects of Na/K ratio

The effects of varying the Na/K ratio of the initial bulk composition are more subtle and somewhat more difficult to evaluate than are the effects due to the H_2O content. There was little morphological difference among the growth patterns exhibited by alkali feldspars which differed in composition by up to 70 mole % $KAlSi_3O_8$. The potassium-rich crystals grew with a slightly more blocky morphology due to a reduction in the growth-rate anisotropy along *c* and *a*, but this observation could not be established quantitatively. The nucleation-density and growth-rate data shown in Figures 12, 13, and 14, reveal only slight differences among the anhydrous compositions. There seems to be no appreciable effect of the Na/K ratio on the nucleation density; the shifts due to H_2O content are reproducible and regular in all of the data, and the minor differences in the absolute magnitudes of the curves for different Na/K ratios are not significant in view of the problems involved in the collection of the raw data.

The only consistent feature which is observed from Figures 12, 13, and 14 is the decrease in the observed growth rates for the Or_{30} compositions relative to those for Or_{10} and Or_{50}. The slight increase in growth rate of the Or_{50} compositions relative to the Or_{10} compositions may be an artifact of the data-collection problems, but the decreases observed near Or_{30} are believed to be significant. The region between roughly 27 and 40 mole % $KAlSi_3O_8$ is a peculiar region in the alkali feldspar system. In this region one finds the solidus minimum, the crest of the alkali feldspar solvus, the room-temeperature monoclinic-triclinic break, and now, a decrease in the observed growth rates from hydrous liquids. These observations suggest that there may be some structural feature, common to both the crystalline and liquid forms of the alkali feldspars which occur in the region where the Na/K ratio approaches 2:1, which is responsible for this behavior. Again, these observations are not pertinent to the results of the present study, but do suggest areas for future study.

The absence of profound effects due to variations in the Na/K ratio of the system was not surprising. The structures of the alkali feldspars, and presumably their liquid counterparts, are not severely affected by the substitution of one alkali for the other, the alumino-silicate network being unaffected chemically and only moderately deformed by this substitution. The bulk of the crystal-growth process is presumably involved in the construction of this framework of tetrahedra, and should not differ significantly over the range of Na/K ratios investigated. Alkali diffusion is sufficiently rapid in these systems (see discussion in next section) that there should be little effect on the kinetics of nucleation and growth, or on the morphology of the resultant crystals.

Crystal-liquid equilibria

In view of the rapid growth rates observed during the present study, it was felt necessary to determine the homogeneity of both the crystals and the coexisting liquids (glasses after quenching). For experiments performed at temperatures above the solidus, the equilibrium crystal-liquid tie-line configuration was also tested. Two techniques have been employed to evaluate these conditions: X-ray powder diffraction analysis of the crystals, and electron microprobe analysis of both the crystals and coexisting glass.

Unit-cell parameters were refined for six crystal-growth samples, and for samples of the

TABLE 2. UNIT CELL-PARAMETERS

Sample #	1314	1539	1527	1516	1554	1520	1792	1711	1713
Anhydrous Composition	Or_{10}	Or_{10}	Or_{10}	Or_{10}	Or_{30}	Or_{30}	Or_{10}	Or_{10}	Or_{10}
Wt. % H_2O	2.6	2.6	2.7	2.7	1.7	1.7	4.9	2.7	5.4
Temp. (°C)	900	900	900	900	900	900	740	740	740
Time (hrs.)	240	48	72	240	240	240	240	48	48
a (Å)	8.172(1)	8.170(1)	8.169(1)	8.170(1)	8.275(1)	8.262(2)	8.197(2)	8.185(1)	8.180(1)
b (Å)	12.892(2)	12.880(2)	12.877(2)	12.880(2)	12.959(3)	12.954(3)	12.883(3)	12.882(1)	12.881(3)
c (Å)	7.119(1)	7.116(1)	7.116(1)	7.116(1)	7.153(1)	7.151(1)	7.133(1)	7.125(1)	7.122(1)
α (°)	93.33(2)	93.38(2)	93.37(1)	93.38(1)	91.50(2)	91.75(3)	93.09(2)	93.24(1)	93.31(2)
β (°)	116.45(1)	116.44(1)	116.44(1)	116.46(1)	116.26(1)	116.28(2)	116.41(2)	116.49(1)	116.47(1)
γ (°)	90.19(2)	90.17(1)	90.16(1)	90.16(1)	90.12(1)	90.13(2)	90.03(2)	90.11(1)	90.14(1)
V (Å^3)	669.9(1)	669.0(1)	668.8(1)	668.9(1)	687.6(2)	685.8(2)	673.5(2)	670.9(1)	670.3(1)
S.E. *	0.013	0.014	0.014	0.016	0.016	0.022	0.024	0.015	0.015
Ref. *	29/29	39/39	40/45	42/43	30/32	34/34	41/44	42/45	43/43
N_{Or}	0.06	0.05	0.05	0.05	0.29	0.27	0.10	0.08	0.07

* S.E. refers to the estimated standard error on a unit weight observation (° 2θ), Ref. refers to the number of peaks used in the refinement/the number of peaks submitted to the program. Numbers in parentheses are the standard errors on the last decimal place.

same bulk composition which were synthesized directly from gels at the identical temperature and pressure conditions as the nucleation and growth step. The powder patterns obtained from the crystal-growth experiments were of excellent quality; in fact the reflections were much sharper and better defined than those from the direct-synthesis experiments. The refined cell parameters are listed in Table 2 and are divided into three groups. The first group is from a series of experiments done on bulk composition number 1. The first refinement listed (sample 1314) was obtained by direct synthesis from a gel at 900°C and 2.5 kbar for 10 days. This sample is defined as the "equilibrium" assemblage of alkali feldspar plus silicate liquid. The other three samples (1539, 1527, and 1516) represent crystals grown from a homogeneous silicate liquid at 900°C and 2.5 kbar for 2, 3, and 10 days respectively. The last row in Table 2 lists the compositions of the feldspars in mole % $KAlSi_3O_8$. These compositions were calculated by averaging the values obtained from three separate determinative curves: 1) the observed position of the ($\bar{2}01$) diffraction maxima were compared to a curve constructed from alkali feldspars crystallized in the subsolidus region from the same gels used throughout this study, 2) the refined values of a were used with the determinative curve based on the sanidine – high albite series of Orville (1967) as fitted by Luth & Querol-Suñé (1970), and 3) the refined unit-cell volumes were compared with a determinative curve from the previous source. All three calculated compositions agreed to within 1 mole % for this first group of refinements.

Note the excellent agreement of the unit-cell parameters among the three crystal-growth samples and their agreement with the direct-synthesis sample. Sample 1314 contained slightly less H_2O than did the other three samples and consequently, its feldspar should be slightly more potassic because of the nature of the tie-lines in this part of the ternary system (see Fig. 1a). As can be seen from Table 2, the first four samples do represent a series of rational two-phase tie lines and thus appear to represent equilibrium assemblages.

The second group of refinements listed in Table 2 is a pair of experiments on bulk composition number 4. The first sample (1554) is the direct-synthesis sample and represents the "equilibrium" assemblage; the second (1520) is the result of a crystal-growth experiment on the same bulk composition. In this instance, the agreement between the refined unit-cell parameters and the calculated compositions of the two samples is not nearly as satisfactory as the first group. As can be seen from the unit-cell standard errors, the overall refinements are poorer, due in part to the inferior quality of the powder patterns obtained from these and all other samples in this compositional range. The poor crystallinity reflected by the quality of the pow-

der patterns may be another indication of the anomalous crystal-chemical behavior of the alkali feldspar series in the compositional range around Or_{30}. The H_2O contents of these two samples were nearly identical, and since the tie-lines in this region of the ternary system do not vary excessively with small changes in H_2O content (see Fig. 1a), the reason for the compositional difference cannot be explained except by disequilibrium effects.

The third group of refinements presented in Table 2 comprise a series of experiments under subsolidus conditions. Had equilibrium been established in these samples, all should be identical and equivalent in composition to the anhydrous bulk composition, Or_{10}. Only the direct-synthesis experiment (sample 1792) fulfills this last criterion. The crystal-growth samples seem to preserve a feldspar-liquid tie-line from some hypersolidus temperature. These charges (1711 and 1713) do contain residual glass (as can be seen in Fig. 7d, which is a duplicate to sample 1711). This preservation of a two-phase tie-line becomes even more obvious when the H_2O contents of the two samples are taken into account; 1711 contains less H_2O and should yield a more potassic feldspar composition, which it does. The temperature equivalent to these tie-line

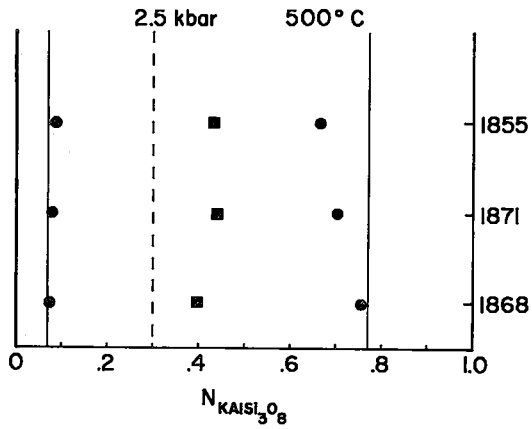

FIG. 15. Alkali feldspar compositions at 500°C and 2.5 kbar within the solvus. Solid circles are observed compositions of the major phases. Solid squares are observed compositions of initial metastable feldspar. Vertical dashed line indicates initial anyhdrous bulk composition and solid vertical lines are the limbs of the "equilibrium" solvus.
Sample 1855: Bulk composition 6 (Or_{30} + 9.5 wt. % H_2O), 72 hrs.
Sample 1871: Bulk composition 6 (Or_{30} + 9.5 wt. % H_2O), 240 hrs.
Sample 1868: Bulk composition 5 (Or_{30} + 4.3 wt. % H_2O), 240 hrs.

orientations cannot be estimated with any degree of certainty, but an examination of the isothermal ternary sections generated during the initial stages of this study indicates that it lies somewhere in the range 770°-800°C. Thus it appears that an alkali feldspar liquid which is quenched rapidly into the subsolidus region will initially crystallize a metastable feldspar-liquid pair, and only upon complete crystallization and homogenization will the equilibrium assemblage be established. A similar effect has been noted in the subsolidus crystallization of alkali feldspars from glasses and gels (Parsons 1969).

Powder patterns, but not unit-cell parameters, were also obtained for a series of samples crystallized from bulk compositions 5 and 6 (Or_{30} + 4.3 and 9.5 wt. % H_2O respectively) at 500°C. This isotherm places the bulk compositions well within the alkali feldspar solvus at the time of crystallization. Data obtained by the direct synthesis of gels at this temperature and pressure were used to locate the limbs of the "equilibrium" solvus for comparison with the results of the crystal-growth experiments. The compositional data obtained from the position of the ($\bar{2}01$) diffraction maximum are plotted on Fig. ure 15. Three distinct ($\bar{2}01$) maxima were observed in the crystal-growth samples, the central peak being of low intensity but easily distinguishable from the other two. Two features are readily apparent from Figure 15. First, the two samples which were identical in composition (1855 and 1871) indicate that the approach to the solvus limbs is enhanced by the longer duration of the nucleation and growth step of sample 1871. This result is not particularly surprising, but it is interesting to note that even after 240 hours the crystal-growth samples have not reached their "equilibrium" positions; this is especially true for the potassic limb. The second feature apparent from Figure 15 is that a comparison of the two samples from experiments of equal duration (1871 and 1868) reveals that the efficiency of the approach to the solvus limbs is apparently inversely proportional to the initial H_2O content of the liquid, a totally unexpected result.

The presence of three alkali feldspars, as revealed by the powder patterns, is related to the previously discussed metastable crystallization of a feldspar-liquid pair under subsolidus conditions. The feldspar compositions derived from the central ($\bar{2}01$) maxima, when combined with the bulk compositions of the samples, yield a rational set of tie-lines in the ternary system. The textural relationships of these three alkali feldspars have not been determined. A typical subsolvus assemblage of individual Na-rich and

K-rich phases would be the expected result, but the presence of an initial homogeneous feldspar of intermediate composition confuses the issue. Should this metastable feldspar be undergoing exsolution, these results would have rather disturbing implications as to the validity of the hypersolvus versus subsolvus classification of granitic rocks. The rather sparse data collected during the present study suggest this possibility, but this aspect of the problem deserves further attention.

Several of the crystal-growth samples were mounted in epoxy and polished for electron microprobe analysis. The major goal was to establish whether the crystals and glasses are chemically homogeneous, or if there are concentration gradients preserved on either side of the interface. Spot analyses were made in several instances to check the X-ray diffraction compositional data. For crystal-growth experiments performed at temperatures above the solidus, the compositional data derived from the microprobe analyses agreed to within 2 mole % $KAlSi_3O_8$ with those obtained by X-ray powder methods. The homogeneity of the initial liquid from which the crystals were nucleated and grown was also checked by rapidly quenching a sample after the homogenization period, and doing several spot analyses across the full sample. No evidence was found for chemical inhomogeneity (but H_2O could not be determined).

The bulk of the microprobe studies involved scans across crystals, glasses, and the interfaces between them. Using a 10 μm beam diameter and a scan rate of 16 μm per minute, no concentration gradients were observed for Na, K, or Al in either the crystals or glasses, and no boundary-layer segregation was observed. The absence of gradients in the alkali elements is not surprising in view of recent diffusion data. The diffusion of alkali elements in crystalline alkali feldspars is relatively rapid (Kasper 1974; Foland 1974) and is evident from the ease with which the alkalis can be exchanged in molten alkali chlorides. Diffusion in the dry alkali feldspar glasses is more rapid than in the crystalline state; in fact, the measured diffusion coefficients for Na and K (Jambon & Carron 1976) are of the same order of magnitude as the growth rates of the alkali feldspars which were measured during the present study. Thus any diffusion layer developed in the liquid would be approximately 1 cm in width (Keith & Padden 1963), which is larger than the sample sizes used in the present experiments. This argument of course ignores the effect of H_2O on the alkali diffusion rates, but it is expected that the addition of H_2O to the liquid would enhance the diffusivities and hence increase the width of the diffusion layer. A wide diffusion layer indicates that any gradients would be low and inhomogeneities in the alkali distributions produced during crystal growth would be quickly erased by the rapid diffusion.

Silicon and aluminum would not be expected to show any diffusion-layer concentration in this system because of the chemical similarity of the crystals and liquid with respect to these elements. The growth process relative to these components is envisaged as a local reconstruction of the tetrahedral framework of the liquid without necessitating any long-range diffusion.

The only component which could not be measured by the present techniques is H_2O. Petrographic observations of several of the samples produced during the present experiments suggest that there is a boundary-layer segregation of H_2O. In charges with a low initial H_2O content, this interface segregation and concentration led to local H_2O saturation at the crystal-liquid interface and the consequent production of non-equilibrium fluid inclusions. These observations have been discussed by Fenn & Luth (1973) and are currently being extended to other compositions.

Applications

Theoretical analysis

The application of the present data to the available theories of nucleation and crystal growth was one of the major goals of the present study. Unfortunately, the problems involved in the collection of accurate rate data using the present experimental techniques have made this application difficult. Even though the general trends of the data conform to those which have been observed or predicted for other silicate systems, the inability to directly observe and therefore accurately measure the process defeats any quantitative application to theory. Even if accurate growth-rate data could be measured for this system, the lack of precise thermochemical data on the phases, especially the liquid, would necessitate certain assumptions which would again invalidate the application. Before any correspondence between the theories and experimentally measured rate-data for hydrous silicate systems can be made, the techniques and technology of the experimental study must be modified to permit the collection of accurate growth-rate data.

Beyond this, there is a critical need for thermochemical and physical data such as heat capacities, viscosities, thermal conductivities, diffusi-

vities, etc., pertinent to the various components and phases which participate in the process. Further experimental work is also needed to define the effects of additional components on the kinetics of the process; Swanson (1976) has shown that the growth rates for alkali feldspars grown from a more complex liquid are considerably lower than those observed in the present study. Once these data are at hand, or can be reasonably estimated, the theories of nucleation and crystal growth can be used in unravelling the cooling histories of natural systems as has been attempted by Kirkpatrick (1976b).

Geochemistry

The ability to synthesize large crystals and equilibrium crystal-liquid pairs opens new possibilities for phase equilibrium and trace and major-element distribution studies. Experimental charges such as those produced during the present study make it possible to perform direct, *in situ* measurements of crystal and liquid compositions using the electron microprobe in systems which previously produced only 10 to 20 μm crystals set in a glassy matrix. Unfortunately, not all systems produce equilibrium crystal-liquid assemblages using the present techniques. Lofgren (1974) has noted the existence of compositional disequilibrium between plagioclase feldspars and coexisting liquids in the system $CaAl_2Si_2O_8$-$NaAlSi_3O_8$-H_2O. Swanson (1974) showed by X-ray powder-diffraction methods that the plagioclase and alkali feldspars grown from a hydrous synthetic granodiorite liquid correspond to those crystallized directly from a gel, but Naney (1975) reported that the addition of mafic components to the same system modifies this behavior. With the addition of biotite components to the liquid, pyroxenes and/or biotite nucleate and grow from the liquid under conditions where the phase-equilibrium data indicate that plagioclase alone should be stable. Such metastable crystallization has been noted in a lunar basaltic vitrophyre (see Brown & Wechsler 1973) and may be an important process in the crystallization of terrestrial rocks. The process of crystallization, whether stable or metastable, can now be studied in the laboratory; crystallization does not have to be reconstructed from the rocks, and the equilibrium phase relations are not restricted only to various stages in the crystallization process.

Trace and major-element distributions between crystals and coexisting silicate liquids have been used in the interpretation of cooling histories for many years. Typically, the trace-element distributions are measured for phenocrysts and compared to those of the groundmass which is assumed to be representative of the liquid phase at the time of crystallization of the phenocrysts. This model implies that, during the cooling and crystallization of the groundmass, there was no re-equilibration with the phenocrysts and the system was closed with respect to the transfer of trace elements from the surrounding environment. Also typically ignored are the kinetic disequilibrium effects discussed and modelled by Albarede & Bottinga (1972). In spite of these difficulties, trace-element partition coefficients have been measured in natural samples and widely used in the interpretation of fractionation and differentiation processes in igneous rocks.

Recently, there have been several attempts to determine partition coefficients experimentally under carefully controlled chemical and physical conditions (for instance see Drake & Weill 1975). Unfortunately, the bulk of these experimental studies has been performed at atmospheric pressure in the absence of H_2O and other volatiles. This limits direct applicability to the dry extrusive rocks. Granitic rocks are not amenable to this type of study because of extreme difficulty in growing crystals from their viscous dry melts. With present techniques, the distribution of trace elements under plutonic conditions can be modelled and the effects of volatile components such as H_2O can be evaluated.

The distribution of major elements among the various phases in a crystal-liquid system has been one of the principal problems investigated by classical phase-equilibrium techniques. Cation distributions between coexisting phases have been used both as geothermometers and geobarometers. Virtually all of these techniques involve the assumption that equilibrium had been established between the phases at the conditions which prevailed during crystallization. Unfortunately, chemical zoning in many of the common rock-forming minerals indicates that such equilibrium is seldom established. As Lofgren (1972) has shown, zoning patterns displayed by plagioclase feldspars can be reproduced experimentally and can be correlated to temperature changes in the system. The ability to examine the kinetics, and the physical and chemical controls on the distribution of the major components in a crystal-magmatic liquid system, may one day allow the petrologist to reveal, from the partitionings and zoning patterns of the major elements, the cooling history of such a system.

Mineralogy

The growth of large single crystals under carefully controlled conditions of temperature,

pressure, and composition will provide the mineralogist-crystallographer with samples of minerals which are not easily obtainable in nature. Many mineral groups, such as the alkali feldspars, are affected by subsolidus chemical and structural variations, including order-disorder and exsolution phenomena. These factors create problems in obtaining chemically intermediate members of solid-solution series, or polymorphs which are stable at high temperatures and/or pressures. Crystal-growth studies performed under magmatic conditions may provide part of the solution. Using a crystal grown by the technique described in the present study, Fenn & Brown (1976) have finished the first study of a homogeneous compositionally intermediate alkali feldspar, and Prewitt *et al.* (1974) have investigated the high-temperature behavior of an intermediate albite crystal grown by Lofgren.

Similar problems exist in the plagioclase feldspars, the pyroxenes, and the amphiboles, to name a few of the common mineral series. These problems may also be amenable to a similar form of attack. The areas of mineralogical research which will benefit from the availability of large single crystals grown under carefully controlled conditions are not as yet fully defined, but the profitable association of the crystal grower and the crystallographer can now be extended to mineral groups previously inaccessible.

Textural development

The textural features displayed by the common igneous rocks are still one of the primary tools of the petrologist in his attempt to reconstruct cooling histories of igneous rocks. The inability of the experimental petrologist to reproduce these textures directly, and the limited applicability of phase-equilibrium data to most natural occurrences, has led to an ever-widening gulf between the experimentalist and the field-based petrologist. The techniques of crystal growth from geologically relevant liquids under magmatic conditions used in the present study, and especially by Lofgren and his coworkers, allow the experimentalist to duplicate these textures and to study the processes involved in textural development.

The results of the present study have little direct application to textural development in common igneous rocks. The experiments were designed to extract quantitative nucleation and growth data from a simple system over a wide range of undercoolings. The experimental cooling rates were far higher than can be reasonably assumed for natural systems, and the isothermal, isobaric nucleation and growth steps are not as satisfactory as controlled cooling-rate experiments in the modelling of natural processes. Perhaps the major weakness of the present data with regard to natural systems is the relative simplicity of the compositions investigated. In this system, the morphological development with increasing undercooling has been shown to be quite simple, but in the plagioclase feldspar series studied by Lofgren (1974), a more complex trend was observed. This variation is undoubtedly due to the extra chemical variable involved in the crystallization process, the coupled substitution of Si and Al with Na and Ca. Swanson (1976) has shown the presence of different morphological trends and a reduction in the observed growth rates in a model granodiorite system, especially when the coprecipitation of two or more phases occurs. Some preliminary data in the system $NaAlSi_3O_8$-SiO_2-H_2O collected by the author indicate that the presence of excess SiO_2 in the liquid modifies the growth morphology of albite from tabular to dendritic at comparable undercoolings. Experiments are underway to determine the effects of a silica deficiency and the presence of boron, fluoride, or chloride in the liquid.

The addition, to the liquid, of components which are not incorporated into the crystal structure can affect the nucleation and growth processes in three basic ways. First, they dilute the system with respect to the components which make up the crystal, thereby necessitating long-range diffusion of several components both toward and away from the crystal-liquid interface. Second, they may modify the structure of the liquid sufficiently to necessitate a major reconstructive change during the crystallization process. Third, if the diffusivities of these components in the liquid are low relative to the growth rate of the crystal, an impurity layer will be built up at the crystal-liquid interface. These three factors are by no means separable from one another; in fact, they are often linked in a causative relationship, and their net effect is typically a reduction in the growth rate and a modification of the growth morphology through an interface breakdown (Keith & Padden 1963). The effects of various system-modifying components must be determined before a quantitative model of textural development can be established and used in a predictive sense.

In spite of these difficulties, the nucleation and growth-rate data presented in Figures 12, 13, and 14 can be used to qualitatively analyze possible textural patterns developed from hydrous silicate melts. Even though the curves as presented are specific for the bulk compositions involved, their general shape and relationship to

one another are felt to be representative of the behavior of other silicate-H_2O systems. The nucleation and growth data for a single bulk composition, such as in Figure 9a, illustrate the relationship of the two curves to the total system undercooling. At low undercoolings the growth rate is low but rapidly increases as the undercooling increases, whereas the nucleation densities remain low until much greater undercoolings. Thus, at an undercooling on the order of 100°C, the texture is dominated by a few rapidly growing crystals. At higher undercoolings, in the neighborhood of 400°C, the system consists of a large number of small equigranular crystals, a texture similar to the groundmass of porphyritic rocks or to aplitic occurrences.

This type of simplified analysis creates a fairly pleasing picture of textural development in a cooling magmatic system, but it must be realized that such an analysis requires that the system achieve its ultimate undercooling rapidly, without any crystallization until the growth temperature is reached. These curves are constructed for a specific bulk composition at set values of the undercooling; if the composition of the liquid changes during the temperature drop to the undercooling values in question, a different set of curves must be used which is appropriate to the new composition. Thus the development of a fine-grained equigranular texture by an argument similar to that used above requires that the liquid be rapidly quenched to an undercooling of roughly 400°C before the onset of crystallization. This process is extremely difficult to envisage in the natural plutonic environment unless the quenching is assumed to be due to a combined pressure and temperature drop on intrusion or, more likely, extrusion. At pressures of 2 to 3 kbar, many H_2O-saturated granitic compositions can be completely melted and homogenized at temperatures around 720°C. If such a system were rapidly brought to the surface before any crystallization could commence, there would be an effective undercooling of some 250°C without any change in the actual temperature of the liquid. This model unfortunately depends heavily upon the H_2O content of the initial liquid; if the initial H_2O content were low and an undersaturated liquid were generated (at a significantly higher temperature than mentioned above), the decrease in pressure would lead to a lowering of the saturation level of the liquid and thereby decrease the liquidus temperature of the system. If this were the case, then a pressure quench would lead to a superheating of the liquid rather than the required supercooling. In analyzing real systems, the chemical effects on the liquidus temperature must be considered as well as the true temperature and pressure variations.

As crystallization proceeds for any system, components such as H_2O which are rejected by the growing crystal will be concentrated in the residual liquid. The effects of this compositional variation on the effective undercooling and crystal morphology have been discussed previously. The rate of decrease of the liquidus temperature, because of this chemical segregation, must be considered in relation to the cooling rate of the entire system. Unless the net cooling rate can match or outstrip the chemical lowering of the liquidus, the undercooling of the system will decrease as crystallization proceeds. To speculate on the role of this process in textural development, the combined nucleation and growth data, such as that shown on Figure 13, must be used. Consider an initial liquid containing 1.7 wt. % H_2O at an undercooling of 50°C. As crystallization proceeds, the H_2O content of the residual liquid will rise, the liquidus temperature will drop, and the undercooling will vary. If the undercooling remains constant or decreases, it can be seen from Figure 13 that both the growth rate and the nucleation density will increase as the H_2O content of the liquid rises. Thus the growth rate of an individual crystal will probably not remain constant with time, and this may affect both the crystal morphology and the distribution of trace and major elements. The problem of achieving equilibrium must also be considered in this type of system. All of these factors must be considered in any analysis of the crystallization of a dynamic system. Other factors, such as the effect of the mutual crystallization of two or more phases which share a common component, cannot be investigated using the present data, but have been considered by Swanson (1976) and represent a fruitful area for further research.

It must be realized that all of the conclusions which may be drawn from such nucleation and growth data may not be the final word on textural development. Subsolidus recrystallization has been shown to have some effect on the experiments done during the present study and may have a much more profound effect in plutonic systems. The nucleation and growth of crystals from the melt may represent only one-quarter of the cooling history of a plutonic body; whether or not the textures developed during this stage will survive through the subsolidus cooling cannot be answered at present. In spite of this problem, the ability to model experimentally the first stages in the crystallization process represents a major step in the analysis of igneous textures.

Conclusion

The results of the present study of the nucleation and growth of alkali feldspars from hydrous melts have presented more problems and asked more questions than have been answered. The ability to grow large crystals, to experimentally model the kinetic processes involved in the crystallization of an igneous rock, and to investigate in detail the controls on textural development represents a new and exciting area of research in experimental petrology. The experimentalist can finally begin to answer the challenges put forth by Iddings nearly 90 years ago and, in doing so, move into a closer association with petrographers and field petrologists. The future of experimental petrology may well lie in the application of the vast amount of phase-equilibrium data to the modelling of the dynamic processes involved in the formation of the igneous rocks. Such an application will involve experiments such as those performed in the present study, and the controlled cooling-rate experiments used by Lofgren. These experiments will give the petrologist an improved insight into the nature of the processes which he has for decades been forced to reconstruct from the final products of these processes, the igneous rocks.

Acknowledgements

The author would like to thank Dr. W. C. Luth for his enthusiastic encouragement throughout the course of the present study. Special thanks are expressed to Peter R. Gordon, without whose technical assistance in the maintenance of the high-pressure apparatus, the present study could not have been performed. The preparation of the manuscript has benefited from discussions with Dr. Samuel E. Swanson and Bernard H. W. S. de Jong. Helpful reviews by Drs. R. James Kirkpatrick and Gary Lofgren have greatly improved the presentation of these results.

Financial support from the National Science Foundation through grants GA 1684 and GA 41731 is gratefully acknowledged.

References

Albarede, F. & Bottinga, Y. (1972): Kinetic disequilibrium in trace element partitioning between phenocrysts and host lava. *Geochim. Cosmochim. Acta* **36**, 141-156.

Brown, G. E. & Wechsler, B. A. (1973): Crystallography of pigeonites from basaltic vitrophyre 15597. *Proc. Fourth Lunar Sci. Conf.* **1**, 887-900.

Brown, S. D. & Ginell, R. (1962): The partial structure of glass and the reconstructive nature of devitrification processes. *In* Symposium on Nucleation and Crystallization in Glasses and Melts (M. K. Reser, G. Smith, H. Insley, eds.), *Amer. Ceramic Soc., Columbus, Ohio,* 109-118.

Crawford, M. L. (1973): Crystallization of plagioclase in mare basalts. *Proc. Fourth Lunar Sci. Conf.* **1**, 705-717.

Daubrée, A. (1857): Observations sur le métamorphisme et recherches expérimentales sur quelques-uns des agents qui ont pu le produire. *Ann. Mines* **12**, 289-326.

——— (1879): *Études Synthétiques de Géologie Expérimentales.* Paris.

Day, A. L. & Allen, E. T. (1905): The isomorphism and thermal properties of the feldspars. Part 1. Thermal study. *Carnegie Inst. Wash. Publ.* **31**, 15-75.

Dietz, E. D., Baak, T. & Blau, H. H. (1970): The superheating of an albite feldspar. *Z. Krist.* **132**, 340-360.

Dowty, E. (1976): Crystal structure and crystal growth: I. The influence of internal structure on morphology. *Amer. Mineral.* **61**, 448-459.

Drake, M. J. & Weill, D. F. (1975): Partition of Sr, Ba, Ca, Y, Eu^{2+}, Eu^{3+}, and other REE between plagioclase feldspar and magmatic liquid: an experimental study. *Geochim. Cosmochim. Acta* **39**, 689-712.

Evans, H. T., Appleman, D. E. & Handwerker, D. S. (1963): The least squares refinement of crystal unit cells with powder diffraction data by an automatic computer indexing method. *Amer. Cryst. Assoc. Ann. Meet. Program* Cambridge, Mass., 42-43 (Abstr.).

Fenn, P. M. (1972): Nucleation and growth of alkali feldspars from synthetic melts. *EØS, Trans. Amer. Geophys. Union* **53**, 1127 (Abstr.).

——— (1974): Nucleation and growth of alkali feldspars from a melt. *In* The Feldspars (W. S. MacKenzie & J. Zussman, eds.), Manchester Univ. Press, Manchester, England, 360-361.

——— & Brown, G. E. (1976): Crystal structure of a synthetic compositionally intermediate alkali feldspar: evidence from Na/K site ordering. *Z. Krist.* (in press).

——— & Luth, W. C. (1973): Hazards in the interpretation of primary fluid inclusions in magmatic minerals. *Geol. Soc. Amer. Program Abstr.* **5**, 617.

Foland, K. A. (1974): Alkali diffusion in orthoclase. *In* Geochemical Transport and Kinetics (A. L. Hofmann, B. J. Giletti, H. S. Yoder, Jr., & R. A. Yund, eds.), *Carnegie Inst. Wash. Publ.* **634**, 77-98.

Fouqué, F. & Michel-Lévy, A. (1882): *Synthèse des Minéraux et des Roches.* Paris.

FRIEDEL, C. & SARASIN, E. (1883): Sur la reproduction de l'albite par voie aqueuse. *Comptes Rendus Acad. Sci. Paris* **97**, 290-294.

GORANSON, R. W. (1938): Silicate-water systems: phase equilibria in the $NaAlSi_3O_8$-H_2O and $KAlSi_3O_8$-H_2O systems at high temperatures and pressures. *Amer. J. Sci.* **35-A**, 71-91.

HALL, J. (1798): Experiments on whinstone and lava. *Trans. Roy. Soc. Edinburgh* **5**, 43-76.

IDDINGS, J. P. (1889): On the crystallizatiton of igneous rocks. *Phil. Soc. Wash. Bull.* **11**, 65-113.

——— (1891): Spherulitic crystallization. *Phil. Soc. Wash. Bull.* **11**, 445-464.

——— (1905): The isomorphism and thermal properties of the feldspars. Part II. Optical study. *Carnegie Inst. Wash. Publ.* **31**, 79-95.

——— (1909): *Igneous Rocks I. Composition, Texture and Classification.* John Wiley & Sons, New York.

JACKSON, K. A., UHLMANN, D. R. & HUNT, J. D. (1967): On the nature of crystal growth from the melt. *J. Crystal Growth* **1**, 1-36.

JAHNS, R. H. & BURNHAM. C. W. (1958): Experimental studies of pegmatite genesis: melting and crystallization of granite and pegmatite. *Bull. Geol. Soc. Amer.* **69**, 1592-1593 (Abstr.).

JAMBON, A. & CARRON, J.-P. (1976): Diffusion of Na, K, Rb and Cs in glasses of albite and orthoclase composition. *Geochim. Cosmochim. Acta* **40**, 897-903.

JONES, G. O. (1971): *Glass.* 2nd ed. Chapman & Hall Ltd., London.

KANI, K. (1935): Viscosity phenomena of the system $KAlSi_3O_8$-$NaAlSi_3O_8$ and of perthite at high temperatures. *Proc. Imp. Acad. Tokyo* **11**, 334-336.

KASPER, R. B. (1974): Cation diffusion in low albite. *Geol. Soc. Amer. Program Abstr.* **6**, 815.

KEITH, H. D. & PADDEN, F. J., JR. (1963): A phenomenological theory of spherulite crystallization. *J. Appl. Phys.* **34**, 2409-2421.

KIRKPATRICK, R. J. (1974): Kinetics of crystal growth in the system $CaMgSi_2O_6$-$CaAl_2SiO_6$. *Amer. J. Sci.* **274**, 215-242.

——— (1975): Crystal growth from the melt: a review. *Amer. Mineral.* **60**, 798-814.

——— (1976a): Measurement and calculation of crystal growth rates in silicate systems. *Geol. Assoc. Can./Mineral. Assoc. Can. Program Abstr.* **1**, 65.

——— (1976b): Towards a kinetic model for thte crystallization of magma bodies. *J. Geophys. Res.* **81**, 2565-2571.

KLEIN, L. & UHLMANN, D. R. (1974): Crystallization behavior of anorthite. *J. Geophys. Res.* **79**, 4869-4874.

LOFGREN, G. E. (1972): Crystallization studies on plagioclase. *EØS, Trans. Amer. Geophys. Union* **53**, 549 (Abstr.).

——— (1973): Experimental crystallization of plagioclase at prescribed cooling rates. *EØS, Trans. Amer. Geophys. Union* **54**, 482 (Abstr.).

——— (1974): An experimental study of plagioclase crystal morphology: isothermal crystallization. *Amer. J. Sci.* **274**, 243-273.

———, DONALDSON, C. H., WILLIAMS, R. J., MULLINS, O. & USSELMAN, T. M. (1974): Experimentally reproduced textures and mineral chemistry of Apollo 15 quartz-normative basalts. *Proc. Fifth Lunar Sci. Conf.* **1**, 549-567.

LUTH, W. C. & INGAMELLS, C. O. (1965): Gel preparation for hydrothermal experimentation. *Amer. Mineral.* **50**, 255-258.

——— & QUEROL-SUNÉ, F. (1970): An alkali feldspar series. *Contr. Mineral. Petrology* **2**, 25-40.

——— & TUTTLE, O. F. (1969): The hydrous vapor phase in equilibrium with granite and granite magmas. *Geol. Soc. Amer. Mem.* **115**, 513-548.

MEILING, G. S. & UHLMANN, D. R. (1967): Crystallization and melting kinetics of sodium disilicate. *Phys. Chem. Glasses* **8**, 62-68.

MEIRS, H. A. & ISSAC, F. (1907): The spontaneous crystallization of binary mixtures. — Experiments on salol and betol. *Proc. Roy. Soc.* **A79**, 322-351.

MUSTART, D. A. (1969): Hydrothermal synthesis of large single crystals of albite and potassium feldspar. *EØS, Trans. Amer. Geophys. Union* **50**. 675 (Abstr.).

NANEY, M. T. (1975): Nucleation and growth of biotite and clinopyroxene from haplogranitic magma. *EØS, Trans. Amer. Geophys. Union* **56**, 1075 (Abstr.).

ORVILLE, P. M. (1967): Unit cell parameters of the microcline-low albite and the sanidine-high albite solid solution series. *Amer. Mineral.* **52**, 55-86.

PARSONS, I. (1969): Subsolidus crystallization behavior in the system $KAlSi_3O_8$-$NaAlSi_3O_8$-H_2O. *Mineral. Mag.* **37**, 173-180.

PREWITT, C. T., SUENO, S. & PAPIKE, J. J. (1974): Models for albite in different structural states. *EØS, Trans. Amer. Geophys. Union* **55**, 464, (Abstr.).

ROGERS, P. S. (1970): The initiation of crystal growth in glasses. *Mineral. Mag.* **37**, 741-758.

SAKKA, S. & MACKENZIE, J. D. (1971): Relation between apparent glass transition temperature and liquidus temperature for inorganic glasses. *J. Non-Crystalline Solids* **6**, 145-162.

SCHAIRER, J. F. (1950): The alkali feldspar join in the system $NaAlSiO_4$-$KAlsiO_4$-SiO_2. *J. Geology* **58**, 512-517.

——— & BOWEN, N. L. (1956): The system Na_2O-Al_2O_3-SiO_2. *Amer. J. Sci.* **254**, 129-195.

SHAW, H. R. (1963): Obsidian-H_2O viscosities at

1000 and 2000 bars in the temperature range 700° to 900°C. *J. Geophys. Res.* 68, 6337-6343.

SWANSON, S. E. (1974): *Phase Equilibria and Crystal Growth in Granodioritic and Related Systems with H_2O and $H_2O + CO_2$.* Ph.D. thesis, Stanford Univ.

——— (1976): Relation of nucleation and crystal growth rate to the development of granitic textures. *Amer. Mineral.* (in press).

TAMMANN, G. (1925): *The States of Aggregation.* D. Van Nostrand Co., New York.

TILLER, W. A. (1970): The use of phase diagrams in solidification. *In* Phase Diagrams, Materials Science and Technology 1 (A. M. Alper, ed.), Academic Press, New York, 199-244.

TURNBULL, D. (1948): Transient nucleation. *Trans. AIME* 175, 774-783.

——— & FISHER, J. C. (1949): Rate of nucleation in condensed systems. *J. Chem. Phys.* 17, 71-73.

VERGANO, P. J., HILL, D. C. & UHLMANN, D. R. (1967): Thermal expansion of feldspar glasses. *J. Amer. Ceramic Soc.* 50, 59-60.

VOLMER, M. & WEBER, A. (1925): Keimbildung in übersättigten gebilden. *Z. Phys. Chem.* 119, 277-301.

WAGSTAFF, F. E. (1968): Crystallization kinetics of internally nucleated vitreous silica. *J. Amer. Ceramic Soc.* 51, 449-452.

WALKER, D., KIRKPATRICK, R. J., LONGHI, J. & HAYS, J. F. (1976): Crystallization history and origin of lunar picritic basalt 12002: phase equilibria, cooling rate studies and physical properties of the parent magma. *Geol. Soc. Amer. Bull.* 87, 646-656.

WINKLER, H. G. F. (1947): Kristallgrösse und abkühlung. *Heidelberger Beitr. Mineral. Petrology* 1, 87-104.

YODER, H. S., Jr. (1950): High-low quartz inversion up to 10,000 bars. *Trans. Amer. Geophys. Union* 31, 827-835.

Manuscript received November 1976, emended February 1977.